



Akbari-Ganji Homotopy Perturbation Method for Analyzing the Pulsatile Blood Flow in Tapered Stenosis Arteries under the Effect of Magnetic Field together with the Impact of Mass and Heat Transfer

Takia Ahmed J. Al-Griffi*, A.S.J. Al-Saif

Department of Mathematics, College of Education for Pure Science, Basrah University, Basrah, Basrah, 61001, Iraq,

Abstract

The two-dimensional pulsatile blood flow in tapered stenosis arteries under the effect of a Magnetic field with mass and heat transfer was analyzed by using a new analytical method called the Akbari-Ganji homotopy perturbation method (AGHPM). This technique is based on integrating the Akbari-Ganji and the homotopy perturbation methods. We succeeded in developing the mathematical model studied by researchers Liu and Liu by adding the effect of the magnetic field of blood flow in addition to the effect of mass and heat transfer on it, this developed model has not been studied before. In the two states (absence and presence) of a magnetic field; the axial velocity, the wall shear stress, flow resistance and volumetric flow rate were investigated under the impact of the angle of tapering, the Grashof number, the solutal Grashof number and magnetic field. The results show that in the case of the absence magnetic field there is good agreement with the previous study made by the researchers Liu and Liu, while in the case of the presence magnetic field it is noted that when the magnetic field increases from 2 to 6, the velocity and flow rate decrease, but in contrast the wall shear stress and resistance flow increases. Moreover, the results establish that AGHPM is effective and extremely accurate in determining the analytical approximate solution for pulsatile blood flow in tapered stenosis arteries under magnetic field influence. Furthermore, the graphs of this novel solution demonstrate the validity, usefulness, and substantiality of AGHPM, and are consistent with the results of earlier investigations.

Keywords: Akbari-Ganji method; blood flow; homotopy perturbation method; tapered stenosis arteries; magnetic field; mass and heat transfer.

1. Main text

The study of bio-fluid dynamics has received a great deal of attention from many researchers and scientists in the last years, especially concerning the facets of the system of human cardiovascular. The source of this tremendous interest is due to the fact that the system of the human cardiovascular is the inner transfer of fluids with multiple offshoots of the arteries along which an intricate flow of blood circulates. There are many different cardiovascular diseases, a stenosis is one of these main diseases that infects the arteries and affects the process of the blood flow.

* Corresponding author.

E-mail address: takiaahmed44@yahoo.com

The stenosis happens in an artery because of the deposit of adipose substances on the internal walls of the artery, a state called atherosclerosis, which leads to the blood flow in the corresponding organs of the body being seriously reduced, resulting in several dangerous circulatory disorders. Because of the importance of studying blood flow in arteries with stenosis, many numbers of researchers and scientists have attempted to find solutions to the problem of blood flow through arteries affected by stenosis (a single case or multiples) by employing various methods for various blood models. For example, Ali et al. [1] solved numerically the blood flow for the Sisko model through a tapered stenosis artery. Chakravarty and Mandal [2] studied the interfering stenosis in an artery for the incompressible Newtonian blood flow model that submitted to body acceleration theoretically. Changdar and De [3] employed the finite difference method for the incompressible viscous unsteady Newtonian fluid model to the blood flow through an artery which has a multiple stenosis. Mandal et al., [4] studied the laminar pulsatile flow of blood through an artery that has stenosis by utilize a finite difference method and beneath the effect of externally imposed periodic body acceleration. Srivastava et al., [5] investigated the blood flow in a two-layered macroscopic model through interfering constriction in the arteries. Zaman et al. [6] analyzed by utilizing a two-dimensional model and in a tapered artery that has stenosis the unsteady pulsatile blood flow, through using a finite difference method. When the physical and medical effects are studied on blood flow, the blood flow system becomes more complicated. Therefore, it is difficult to find exact solutions for this system to clarify these effects, and therefore many researchers resort to searching for a suitable simulation technique to hold their goals. Dada and Alamu-Awoniran [7] studied analytically the impact of heat and mass transfer in flow of blood. They assumed blood to be a micropolar, incompressible fluid through a tapered artery with mild stenosis. Shit and Majee [8] examined unsteady blood flow and heat transfer properties for the Newtonian, incompressible, fluid model in a tapered artery under the existence of whole body vibration and a magnetic field. Shaw et al., [9] treated the blood flow as a Casson fluid model through an artery that has stenosis under the effect of an exterior magnetic field with body acceleration. Sharma and Gaur [10] analyzed the blood flow through arterial catheterization when the blood is exemplified by a Newtonian fluid with the effect of a magnetic field. Ponalagusamy and Priyadharshini [11] processed the blood flow as a Herschel-Bulkley fluid and studied the impact of the existence of a magnetic field and body force through an artery with stenosis. Tripathi and Sharma [12] inspected the impact of mass and heat transfer on the flow of blood under the effect of a magnetic field with a chemical reaction for a non-tapered artery with mild stenosis. Ellahi et al. [13] examined the blood as a fluid flow of Jeffrey in a catheterized tapered artery and they studied the impact of heat transfer with a catheter. Danesh et al. [14] used nonlocal elasticity theory to study the small scale impact on the axial vibration of a tapered nanorod. To analyze the mechanical behavior of nanoscale materials the nonlocal elasticity theory was used. By using the differential quadrature method the governing equations of the nanorod for clamped-clamped, clamped-free and fixed-attached spring boundary conditions were solved. Faghiri et al. [15] examined the Graetz-Nusselt problem for blood as a non-Newtonian fluid. By using the separation of variables method the energy equation is treated after the flow field is identified by solving the momentum and the continuity equations. Moreover, an approximate analytical solution is determined, using an integrated approach to solving boundary layer equations. Finally, the effects of controlling parameters such as surface heat flux and energy law index on the thermal properties of the flow and structure of non-Newtonian fluids are discussed in detail. Hosseinzadeh [16] studied the magnetohydrodynamic (MHD) flow in the presence of microorganisms and nanoparticles on a surface. The impact of thermal radiation, Brownian motion, Magnetic field, Schmidt number, Peclet number, thermophoresis, and bioconvection Schmidt number is investigated. The governing equations are transformed into the ordinary differential equation and then are solved with MAPLE software by taking advantage of the Runge-Kutta fifth-order method. Furthermore, many studies have investigated the impact of magnetic fields on the flow of blood in an artery with stenosis (one instance or several instances) on the different fluid models [17-57]. In 1992, Luo and Kuang [58] suggested a new constitutive equation to describe the shear thinning demeanor for blood at high and low shear rates for the non-Newtonian fluid model. This model is called the K-L model. Additionally, Luo and Kuang conducted an experimental investigation using the K-L model. Results indicated that the K-L model has good agreement with experimental data, and can be utilized to describe blood flow. They deduce that the suggested model is more efficacious in describing shear thinning for the blood flow behavior in comparison with the Newtonian and Casson's models. In 2020, Liu and Liu [59] considered the blood flow as a K-L model and examined the impact of mass and heat transfer on it. Also, they studied the properties of the blood flow.

What was introduced above reflects the importance of studying the flow problem of blood, in addition to the study of the effect of a magnetic field on it, by researchers in various mediums, treating it with various simulation methods. Furthermore based on the information and to the best of our knowledge, the merging process between analytical approaches and approximate methods may alleviate or decrease many of the restrictions associated with handling each method separately. This reason stimulates us to combine the two methods in this study. The first is the analytical method known as the Akbari-Ganji's method (AGM), which is a new method presented by Ganji and

Akbari and may be used to solve a variety of nonlinear differential equations (ordinary and partial). And the second is the homotopy perturbation approach that is discovered by Aminikhah and Hemmatnezhad [60], which is a semi-analytical (approximate) method that takes on a fresh format for the standard homotopy perturbation method (HPM). The combination between these two methods (AGM and HPM) yields an innovative approach known as the Akbari-Ganji's homotopy perturbation method (AGHPM). For these reasons and what has been presented in the historical review above, we were encouraged to do the following: first, the blood is assumed to be a K-L model. Second, we developed the model of blood flow in [59] by adding the effect of a magnetic field in addition to the impact of the heat and mass transfer for the blood flow. According to the information available to us, the new system has not been studied before, and thus will be one of the new innovative points of our work. Third, we use the Laplace transform (LT) and Yang transform (YT) to convert the partial equations of pulsatile blood flow to an ordinary differential equations. Fourth, we resolve the new system by using the new method (AGHPM). Fifth, we study the effect of the magnetic field as well as the properties of blood on the axial velocity, volumetric flow rate, wall shear stress and the flow resistance profile. Finally, we made a comparison between the results obtained by AGHPM, AGM and HPM with and without the existence of the magnetic field. Furthermore, the innovative method could be an improvement for AGM and HPM. The numerical results, obtained by using AGHPM to solve the current problem confirm that the proposed method is competent, effective, and has high precision. And also, its results are in agreement with those are reported by other researchers [59, 61, 62].

The novelty of the current paper lies in the development of the mathematical model that was solved by the researchers in [59] by adding the effect of the magnetic field to it. Moreover; we have solved the current problem under study by using a developed and novel method that has not been used before to solve this problem in two cases, the presence and absence of the effect of the magnetic field. This method give new and high-accuracy results that have been confirmed its validity by comparison with previous studies in the literature, while the limitations of this method are that it can be easily applied to the ordinary differential equation but on the partial differential equation must be firstly transform it into the ordinary differential equation and then applied this method on it. Moreover, this new study (i.e. add effect of the magnetic field) with the applications of (mass and heat transfer) explains the importance of applying the magnetic field and how doctors can benefit from it to reduce the risk of diseases, when used appropriately.

2. The AGHPM Algorithm

The basic idea of the AGHPM is based on the AGM and HPM algorithms, which will be discussed in this section.

2.1. Akbari-Ganji's Method (AGM)

This method was proposed by Akbari and Ganji [63] and it is a very suitable calculation technique that may be used to solve different nonlinear differential equations. In this method the solution is assumed as finite series, so the solution is found by solving a set of algebraic equations.

To apply AGM, the differential equation for a function $U(y)$ and its derivatives can be expressed as follows;

$$p_k = f(U, U', U'', \dots, U^{(m)}) = 0, \quad U = U(y) \quad (1)$$

where p_k is the nonlinear differential equation of m^{th} -order derivatives, with boundary conditions:

$$U(y) = U_0, U'(y) = U_1, \dots, U^{(m-1)}(y) = U_{m-1} \quad \text{at } y = 0 \quad (2a)$$

$$U(y) = U_{L_0}, U'(y) = U_{L_1}, \dots, U^{(m-1)}(y) = U_{L_{m-1}} \quad \text{at } y = L \quad (2b)$$

To solve Equation (1) in connection with the conditions (2a and 2b), the solution of the differential equation is considered as follows;

$$U(y) = \sum_{i=0}^n a_i y^i = a_0 + a_1 y + \dots + a_n y^n \quad (3)$$

By the choosing more terms of Equation (3) leads to a more accurate solution to Equation (1). To obtain the solution for the differential Equation (1), if the series (3) is of (n) degree, then exist $(n+1)$ unknown coefficients, which are need $(n+1)$ equations to be defined. The boundary conditions (2a) and (2b) are applied for Equation (3) as follows:

(a) At $y = 0$, we have the following,

$$\begin{cases} U(0) = a_0 = U_0 \\ U'(0) = a_1 = U_1 \\ U''(0) = a_2 = U_2 \\ \vdots \end{cases} \quad (4)$$

$$\text{when } y = L; \begin{cases} U(L) = a_0 + a_1 L + \dots + a_n L^n = U_{L_0} \\ U'(L) = a_1 + 2a_2 L + \dots + n a_n L^{n-1} = U_{L_1} \\ U''(L) = 2a_2 + 6a_3 L + \dots + n(n-1) a_n L^{n-2} = U_{L_2} \\ \vdots \end{cases} \quad (5)$$

(b) After substituting Equation (3) into Equation (1) and after that we apply the boundary condition to it, we obtain:

$$\begin{aligned} p_0 &= f(U(0), U'(0), U''(0), \dots, U^{(m)}(0)) \\ p_1 &= f(U(L), U'(L), U''(L), \dots, U^{(m)}(L)) \\ &\vdots \end{aligned} \quad (6)$$

With regarding the choice of n ; ($n < m$) the terms in Equation (3) and to making in order a set of equations consisting of $(n+1)$ unknowns and $(n+1)$ equations, we are faced with an additional number of unknowns that are surely the same as the coefficients of Equation (3), so, to overcome on this problem, we must derivate Equation (1) of m time according to the unknowns additional in the set of differential equations above and after that we apply the boundary conditions on it as follows:

$$\begin{aligned} p'_k &: f(U', U'', U''', \dots, U^{(m+1)}) \\ p''_k &: f(U'', U''', U'''' , \dots, U^{(m+2)}) \\ &\vdots \end{aligned} \quad (7)$$

(c) The boundary conditions are applied to Equation (7) as follows:

$$p'_k : \begin{cases} f(U'(0), U''(0), U'''(0), \dots, U^{(m+1)}(0)) \\ f(U'(L), U''(L), U'''(L), \dots, U^{(m+1)}(L)) \end{cases} \quad (8)$$

$$p''_k : \begin{cases} f(U''(0), U'''(0), U''''(0), \dots, U^{(m+2)}(0)) \\ f(U''(L), U'''(L), U''''(L), \dots, U^{(m+2)}(L)) \end{cases} \quad (9)$$

From Equations (4) to (9), $(n+1)$ equations may be worked out, and so $(n+1)$ unknown coefficients of Equation (3) such as $a_0, a_1, a_2, \dots, a_n$ can be computed. By locating the coefficients of Equation (3), the solution to the nonlinear differential Equation (1) will be achieved.

2.2. Homotopy Perturbation Method (HPM)

A fresh form of homotopy perturbation method was found-out by the two scientists Aminikhah and Hemmatnezhad [60] to obtain an analytical solution for the nonlinear differential equations. It is assumed that the solution in this method is an infinite series. To illustrate the basic ideas of this technique [60, 64], let us contemplate the following nonlinear differential equation:

$$A(U(y)) - f(r(y)) = 0 \quad , \quad r(y) \in \Omega \quad (10)$$

with the boundary condition:

$$B\left(U(y), \frac{\partial U(y)}{\partial n}\right) = 0 \quad , \quad r(y) \in \Gamma \quad , \tag{11}$$

where A is a public differential operator, B is the operator of a boundaries, $f(r(y))$ is an analytic well-known function and Γ is the boundary for the domain Ω . The operator A can be divided into two parts, L and N , where L is a linear operator and N is a nonlinear operator. Therefore, Equation (10) can be rewritten as:

$$L(U(y)) + N(U(y)) - f(r(y)) = 0 \tag{12}$$

By the technique of homotopy, we are building a homotopy $v(r, p) : \Omega \times [0,1] \rightarrow \mathbb{R}$ which satisfies:

$$H(v(y), p) = (1 - p)[L(v(y)) - U_0(y)] + p[A(v(y)) - f(r(y))] = 0, \quad p \in [0,1], r(y) \in \Omega, \tag{13}$$

$$\text{or } H(v(y), p) = L(v(y)) - U_0(y) + p[U_0(y) + N(v(y)) - f(r(y))] = 0, \tag{14}$$

where $p \in [0,1]$ is an embedding parameter, $U_0(y)$ is an initial approximation of Equation (10). From Equations (13) and (14), we obtained;

$$H(v(y), 0) = L(v(y)) - U_0(y) = 0 \quad , \tag{15}$$

$$H(v(y), 1) = L(v(y)) + N(v(y)) - f(r(y)) = 0. \tag{16}$$

According to HPM, we can first use the embedding parameter p as a small parameter, and assume that the solutions of Equations (13) and (14) can be represented as a power series in p as follows:

$$v(y) = \sum_{k=0}^{\infty} p^k v_k \tag{17}$$

Let's now rewrite Equation (14) in the following format:

$$L(v(y)) - U_0(y) + p[f(r(y)) - N(v(y)) - U_0(y)] = 0 \tag{18}$$

By applying the inverse operator L^{-1} to both sides of Equation (18), we obtain:

$$v(y) = L^{-1}(U_0(y)) + p \left[L^{-1}(f(r(y))) + L^{-1}(N(v(y))) - L^{-1}(U_0(y)) \right] \tag{19}$$

Assuming the initial approximate of Equation (10) has the following format:

$$U_0(y) = \sum_{k=0}^{\infty} b_k g_k(y) \tag{20}$$

where b_0, b_1, b_2, \dots are unknown coefficients and $g_0(y), g_1(y), g_2(y), \dots$ are specified functions depended on the problem. Now by substituting (17) and (20) into the Equation (19), we have

$$\sum_{k=0}^{\infty} p^k v_k(y) = L^{-1}\left(\sum_{k=0}^{\infty} b_k g_k(y)\right) + p \left[L^{-1}(f(r(y))) + L^{-1}\left(N\left(\sum_{k=0}^{\infty} p^k v_k(y)\right)\right) - L^{-1}\left(\sum_{k=0}^{\infty} b_k g_k(y)\right) \right] \tag{21}$$

By equalizing the coefficients for terms that have the same power p , leads to

$$\begin{aligned}
p^0 : v_0(y) &= L^{-1} \left(\sum_{k=0}^{\infty} b_k g_k(y) \right) \\
p^1 : v_1(y) &= L^{-1} (f(r(y))) - L^{-1} \left(\sum_{k=0}^{\infty} b_k g_k(y) \right) - L^{-1} (N(v_0(y))) \\
p^2 : v_2(y) &= -L^{-1} (N(v_0(y), v_1(y))) \\
&\vdots \\
p^j : v_j(y) &= -L^{-1} (N(v_0(y), v_1(y), \dots, v_{j-1}(y)))
\end{aligned} \tag{22}$$

Therefore, we can obtain the solution as follows:

$$U(y) = v_0(y) = L^{-1} \left(\sum_{k=0}^{\infty} b_k g_k(y) \right) \tag{23}$$

2.3. The Fundamental Notion of the Innovative Method (AGHPM)

To describe the essential notion of the new technique for Equation (12) with conditions (11) is as the following steps:

Step1: By the HPM, we have:

$$L(v(y)) - U_0(y) + p(U_0(y)) + p[N(v(y)) - f(r(y))] = 0, \tag{24}$$

where; $U_0(y)$ is an initial approximate for Equation (10).

Step2: Lets $v(y) = \sum_{i=0}^n a_i y^i = a_0 + a_1 y + \dots + a_n y^n$ and $U_0(y) = \sum_{k=0}^{\infty} b_k g_k(y)$.

Step3: Applying the boundary conditions to the function $v(y)$.

Step4: By putting $v(y)$ and $U_0(y)$ in Equation (24), we have:

$$L \left(\sum_{i=0}^n a_i y^i \right) - \sum_{k=0}^{\infty} b_k g_k(y) + p \left(\sum_{k=0}^{\infty} b_k g_k(y) \right) + p \left[N \left(\sum_{i=0}^n a_i y^i \right) - f(r(y)) \right] = 0 \tag{25}$$

Step5: Equalize the terms that have the same power of p , we obtain:

$$\begin{aligned}
p^0 : v_0(y) &= L \left(\sum_{i=0}^n a_i y^i \right) - \sum_{k=0}^{\infty} b_k g_k(y) \\
p^1 : v_1(y) &= \sum_{k=0}^{\infty} b_k g_k(y) + \left[N \left(\sum_{i=0}^n a_i y^i \right) - f(r(y)) \right] \\
&\vdots
\end{aligned} \tag{26}$$

So on.

Step6: By applying the boundary conditions to Equations (26) to find the unknown coefficients a_i and b_k .

Step7: The analytical solution can be found by putting a_i in:

$$v(y) = \sum_{i=0}^n a_i y^i = a_0 + a_1 y + \dots + a_n y^n .$$

3. Governing equations

3.1. The geometry of stenosis

It is assumed that the artery is a tapered, cylindrical, elastic and thin tube. It has interfering stenosis in the vessel axisymmetric. Cylindrical polar coordinates were used to clarify the blood artery and indicate the point in the system with (r, θ, z) , where: θ and r are circumferential and radial directions respectively, the z -axis is along the axis

of the artery. The geometric shape of the tapered artery with multiple stenosis is shown in Fig. 1:

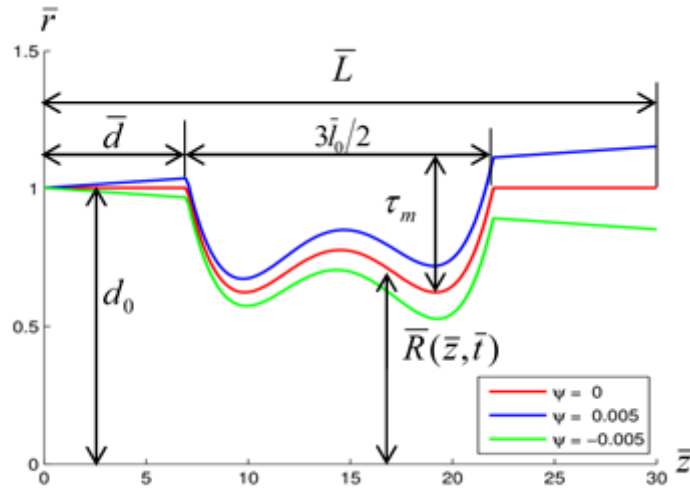


Fig 1: Geometric shape of the tapering artery with stenosis,

and the geometry function as [59]:

$$\bar{R}(\bar{z}, \bar{t}) = \begin{cases} \left([m\bar{z} + d_0] - \frac{\tau_m \cos(\psi)(\bar{z} - \bar{d})}{\bar{l}_0} \bar{\zeta} \right) \bar{a}_1(\bar{t}), & \bar{d} \leq \bar{z} \leq \bar{d} + \frac{3}{2}\bar{l}_0, \\ [m\bar{z} + d_0] \bar{a}_1(\bar{t}), & \text{otherwise,} \end{cases}$$

where: $\bar{\zeta} = 11 - \frac{94(\bar{z} - \bar{d})}{3\bar{l}_0} + \frac{32(\bar{z} - \bar{d})^2}{\bar{l}_0^2} - \frac{32(\bar{z} - \bar{d})^3}{3\bar{l}_0^3}$, $m = \tan(\psi)$ which is the slope of the tapered

vessel. The time-variant parameter is $\bar{a}_1(\bar{t}) = 1 + k \cos(\bar{\omega}\bar{t} - \phi)$, where k indicates some parameter associated with amplitude.

3.2. The equations of the flow

Keep in mind that blood flow is a pulsating fluid in tapered stenosis arteries beneath the influence of a magnetic field combined with the effects of mass and heat transfer, and the blood is bound in the form of a viscous, incompressible fluid. Therefore, with these assumptions, the governing equations (continuity, momentum, energy, and mass concentration) can be written as:

$$\frac{\partial \bar{u}}{\partial \bar{r}} + \frac{\bar{u}}{\bar{r}} + \frac{\partial \bar{w}}{\partial \bar{z}} = 0, \tag{27}$$

$$\rho \left(\frac{\partial \bar{u}}{\partial \bar{t}} + \bar{u} \frac{\partial \bar{u}}{\partial \bar{r}} + \bar{w} \frac{\partial \bar{u}}{\partial \bar{z}} \right) = -\frac{\partial \bar{P}}{\partial \bar{r}} + \left(\frac{1}{\bar{r}} \frac{\partial}{\partial \bar{r}} (\bar{r} \bar{\tau}_{rr}) + \frac{\partial}{\partial \bar{r}} \bar{\tau}_{rz} \right), \tag{28}$$

$$\rho \left(\frac{\partial \bar{w}}{\partial \bar{t}} + \bar{w} \frac{\partial \bar{w}}{\partial \bar{r}} + \bar{w} \frac{\partial \bar{w}}{\partial \bar{z}} \right) = -\frac{\partial \bar{P}}{\partial \bar{z}} + \left(\frac{1}{\bar{r}} \frac{\partial}{\partial \bar{r}} (\bar{r} \bar{\tau}_{rz}) + \frac{\partial}{\partial \bar{r}} \bar{\tau}_{zz} \right) + \rho \bar{\alpha} \bar{g} (\bar{T} - \bar{T}_0) + \rho \bar{\alpha} \bar{g} (\bar{C} - \bar{C}_0) + J \times B, \tag{29}$$

$$\rho c_p \left(\frac{\partial \bar{T}}{\partial \bar{t}} + \bar{u} \frac{\partial \bar{T}}{\partial \bar{r}} + \bar{w} \frac{\partial \bar{T}}{\partial \bar{z}} \right) = \bar{\tau}_{rr} \frac{\partial \bar{u}}{\partial \bar{r}} + \bar{\tau}_{rz} \frac{\partial \bar{w}}{\partial \bar{r}} + \bar{\tau}_{rz} \frac{\partial \bar{u}}{\partial \bar{z}} + \bar{\tau}_{zz} \frac{\partial \bar{w}}{\partial \bar{z}} + k^* \left(\frac{\partial^2 \bar{T}}{\partial \bar{r}^2} + \frac{1}{\bar{r}} \frac{\partial \bar{T}}{\partial \bar{r}} + \frac{\partial^2 \bar{T}}{\partial \bar{z}^2} \right), \tag{30}$$

$$\left(\frac{\partial \bar{C}}{\partial \bar{t}} + \bar{u} \frac{\partial \bar{C}}{\partial \bar{r}} + \bar{w} \frac{\partial \bar{C}}{\partial \bar{z}} \right) = D \left(\frac{\partial^2 \bar{C}}{\partial \bar{r}^2} + \frac{1}{\bar{r}} \frac{\partial \bar{C}}{\partial \bar{r}} + \frac{\partial^2 \bar{C}}{\partial \bar{z}^2} \right) + \frac{DK_T}{T_m} \left(\frac{\partial^2 \bar{T}}{\partial \bar{r}^2} + \frac{1}{\bar{r}} \frac{\partial \bar{T}}{\partial \bar{r}} + \frac{\partial^2 \bar{T}}{\partial \bar{z}^2} \right), \tag{31}$$

where: $B = B_0 + B_1$ is the total magnetic field where B_0 is the exterior magnetic field which is justified for magneto-hydrodynamics (MHD) flow at a small magnetic Reynolds number and B_1 is the induced magnetic field which is negligible.

From Ohm's law [61], we get:

$$J = \sigma(E + V \times B), \quad (32)$$

where; $V = (\bar{u}, 0, \bar{w})$ are the velocity components. The force $J \times B$ can be simplified to:

$$J \times B = -\sigma B^2 V. \quad (33)$$

By putting Equation (33) into Equation (29); then Equation (29) becomes:

$$\rho \left(\frac{\partial \bar{w}}{\partial \bar{t}} + \bar{w} \frac{\partial \bar{w}}{\partial \bar{r}} + \bar{w} \frac{\partial \bar{w}}{\partial \bar{z}} \right) = -\frac{\partial \bar{P}}{\partial \bar{z}} + \left(\frac{1}{\bar{r}} \frac{\partial}{\partial \bar{r}} (\bar{r} \bar{\tau}_{rz}) + \frac{\partial}{\partial \bar{r}} \bar{\tau}_{zz} \right) + \rho \bar{\alpha} \bar{g} (\bar{T} - \bar{T}_0) + \rho \bar{\alpha} \bar{g} (\bar{C} - \bar{C}_0) - \sigma B_0^2 \bar{w}, \quad (34)$$

Where [71]: $\bar{\tau}_{zz} = 2\bar{\eta}(\bar{\gamma}) \left(\frac{\partial \bar{w}}{\partial \bar{z}} \right)$, $\bar{\tau}_{rr} = 2\bar{\eta}(\bar{\gamma}) \left(\frac{\partial \bar{u}}{\partial \bar{r}} \right)$, $\bar{\tau}_{rz} = \bar{\eta}(\bar{\gamma}) \left(\frac{\partial \bar{w}}{\partial \bar{r}} + \frac{\partial \bar{u}}{\partial \bar{z}} \right)$; and $\bar{\eta}(\bar{\gamma}) = \frac{\bar{\tau}}{\bar{\gamma}}$ denotes the apparent viscosity and $\bar{\tau}$ defined as a K-L model.

Since the blood flow is considered pulsatile, so the pressure gradient can be defined as follows [59]:

$$-\frac{\partial \bar{P}}{\partial \bar{z}} = \bar{A}_0 + \bar{A}_1 \cos(\bar{\omega} \bar{t}); \quad t > 0,$$

\bar{A}_0 indicates the amplitude in the state of the steady state, \bar{A}_1 symbolizes the amplitude in the state of the pulsatile blood flow and $\bar{\omega} = 2\pi \bar{f}_p$ is the frequency angular where \bar{f}_p is the pulse frequency.

4. The dimensionless set

Mediate the dimensionless set, defined as follows:

$$r = \frac{\bar{r}}{d_0}, \quad z = \frac{\bar{z}}{d_0}, \quad R = \frac{\bar{R}}{d_0}, \quad u = \frac{\bar{u}}{u_0}, \quad w = \frac{\bar{w}}{u_0}, \quad t = \bar{\omega} \bar{t}, \quad P = \frac{d_0}{u_0 \eta_1} \bar{P}, \quad \tau_0 = \frac{d_0}{u_0 \eta_1} \bar{\tau}_0, \quad \tau_{rr} = \frac{d_0}{u_0 \eta_1} \bar{\tau}_{rr},$$

$$\tau_{zz} = \frac{d_0}{u_0 \eta_1} \bar{\tau}_{zz}, \quad \tau_{rz} = \frac{d_0}{u_0 \eta_1} \bar{\tau}_{rz}, \quad \alpha^2 = \frac{\rho \bar{\omega} d_0^2}{\eta_1}, \quad T = \frac{\bar{T} - \bar{T}_0}{\bar{T}_0}, \quad C = \frac{\bar{C} - \bar{C}_0}{\bar{C}_0}, \quad \text{Re} = \frac{\rho u_0 d_0}{\eta_1},$$

$$E_c = \frac{u_0^2}{c_p \bar{T}_0}, \quad \text{Pr} = \frac{c_p \eta_1}{k^*}, \quad S_r = \frac{\rho D K_T \bar{T}_0}{\eta_1 \bar{C}_0 T_m}, \quad S_c = \frac{\eta_1}{D \rho}, \quad G_r = \frac{g \bar{\alpha} d_0^3 \bar{T}_0}{\eta_1^2}, \quad G_c = \frac{g \bar{\alpha} d_0^3 \bar{C}_0}{\eta_1^2},$$

$$A_0 = \frac{d_0^2}{\eta_1 u_0} \bar{A}_0, \quad A_1 = \frac{d_0^2}{\eta_1 u_0} \bar{A}_1, \quad M = B_0 d_0 \sqrt{\frac{\sigma}{\rho u_0}},$$

So, the Equations (27, 28, 30, 31, 34) can be written in dimensionless as:

$$\frac{\partial u}{\partial r} + \frac{u}{r} + \frac{\partial w}{\partial z} = 0, \quad (35)$$

$$\alpha^2 \frac{\partial u}{\partial t} + \text{Re} \left(u \frac{\partial u}{\partial r} + w \frac{\partial u}{\partial z} \right) = -\frac{\partial P}{\partial r} + \left(\frac{1}{r} \frac{\partial}{\partial r} (r \tau_{rr}) + \frac{\partial}{\partial r} \tau_{rz} \right), \quad (36)$$

$$\alpha^2 \frac{\partial w}{\partial t} + \text{Re} \left(u \frac{\partial w}{\partial r} + w \frac{\partial w}{\partial z} \right) = -\frac{\partial P}{\partial z} + \left(\frac{1}{r} \frac{\partial}{\partial r} (r \tau_{rz}) + \frac{\partial}{\partial z} \tau_{zz} \right) + G_r T + G_c C - \frac{M^2}{\text{Re}} w, \quad (37)$$

$$\alpha^2 \frac{\partial T}{\partial t} + \text{Re} \left(u \frac{\partial T}{\partial r} + w \frac{\partial T}{\partial z} \right) = E_c \left(\tau_{rr} \frac{\partial u}{\partial r} + \tau_{rz} \frac{\partial w}{\partial r} + \tau_{rz} \frac{\partial u}{\partial z} + \tau_{zz} \frac{\partial w}{\partial z} \right) + \frac{1}{\text{Pr}} \left(\frac{\partial^2 T}{\partial r^2} + \frac{1}{r} \frac{\partial T}{\partial r} + \frac{\partial^2 T}{\partial z^2} \right), \quad (38)$$

$$\alpha^2 \frac{\partial C}{\partial t} + \text{Re} \left(u \frac{\partial C}{\partial r} + w \frac{\partial C}{\partial z} \right) = \frac{1}{S_c} \left(\frac{\partial^2 C}{\partial r^2} + \frac{1}{r} \frac{\partial C}{\partial r} + \frac{\partial^2 C}{\partial z^2} \right) + S_r \left(\frac{\partial^2 T}{\partial r^2} + \frac{1}{r} \frac{\partial T}{\partial r} + \frac{\partial^2 T}{\partial z^2} \right). \quad (39)$$

And

$$\tau_{zz} = 2\eta(\gamma) \left(\frac{\partial w}{\partial z} \right), \tau_{rr} = 2\eta(\gamma) \left(\frac{\partial u}{\partial r} \right), \tau_{rz} = \eta(\gamma) \left(\frac{\partial w}{\partial r} + \frac{\partial u}{\partial z} \right); \eta(\gamma) = \frac{\tau_0 + l^* \gamma^{1/2} + \gamma}{\gamma}; l^* = \frac{\eta_2}{\eta_1} \left(\frac{d_0}{u_0} \right)^{1/2},$$

where: $\gamma = 2 \left[\left(\frac{\partial u}{\partial r} \right)^2 + \left(\frac{u}{r} \right)^2 + \left(\frac{\partial w}{\partial z} \right)^2 \right] + \left(\frac{\partial u}{\partial z} + \frac{\partial w}{\partial r} \right)^2$ and η_2 is a chemical variable.

The non- dimensional pressure is defined as [59]

$$-\frac{\partial P}{\partial z} = A_0 + A_1 \cos(\omega t); \quad t > 0.$$

The initial conditions can be defined as:

$$w(r, z, 0) = \left(\frac{A_0 + A_1}{4} \right) \left(1 - \left[\frac{r}{d_0} \right]^2 \right), \text{ in the absence of a magnetic field,}$$

$$w(r, z, 0) = \left(\frac{A_0 + A_1}{M^2} \right) \left(1 - \left[\frac{I_0(rM)}{I_0(M)} \right]^2 \right), \text{ in the presence of a magnetic field,}$$

$$T(r, z, 0) = 0, u(r, z, 0) = 0, C(r, z, 0) = 0,$$

The boundary conditions can be described as follows:

The axial velocity gradient, radial velocity, temperature gradient, and mass gradient are all zero along the axis of symmetry, i.e.

$$\frac{\partial w}{\partial r}(r, z, t) = 0, u(r, z, t) = 0, \frac{\partial C}{\partial r}(r, z, t) = 0, \frac{\partial T}{\partial r}(r, z, t) = 0, \text{ at } r = 0.$$

And at the wall, axial velocity is zero, radial velocity is equal to the artery wall velocity owing to wall motion, temperature and mass are both zero, and these conditions are described as,

$$w(r, z, t) = 0, u(r, z, t) = \frac{\partial R}{\partial t}, C(r, z, t) = 0, T(r, z, t) = 0, \text{ at } r = R(z, t).$$

Also, the non-dimensional form for the geometry of stenosis is as follows:

$$R(z, t) = \begin{cases} \left[[m z + d_0] - \frac{\tau_m \cos(\psi)(z-d)}{l_0} \zeta \right] a_1(t), & d \leq z \leq d + \frac{3}{2} l_0, \\ [m z + d_0] a_1(t), & \text{otherwise,} \end{cases}$$

where: $\zeta = 11 - \frac{94(z-d)}{3l_0} + \frac{32(z-d)^2}{l_0^2} - \frac{32(z-d)^3}{3l_0^3}$ and $a_1(t) = 1 + k \cos(\omega t - \phi)$.

Now, to transmute the governing Equations (35) and (36-39) for the radial coordinates, let $\zeta = \frac{r}{R(z,t)}$, then have:

$$\frac{1}{R} \frac{\partial u}{\partial \zeta} + \frac{u}{\zeta R} + \frac{\partial w}{\partial z} - \frac{\zeta}{R} \frac{\partial R}{\partial z} \frac{\partial w}{\partial \zeta} = 0, \quad (40)$$

$$\begin{aligned} \frac{\partial w}{\partial t} = & \frac{\zeta}{R} \frac{\partial R}{\partial t} \frac{\partial w}{\partial \zeta} + \frac{\text{Re}}{\alpha^2} \left(-\frac{u}{R} \frac{\partial w}{\partial \zeta} + \frac{\zeta}{R} \frac{\partial R}{\partial z} \frac{\partial w}{\partial \zeta} w - w \frac{\partial w}{\partial \zeta} \right) - \frac{1}{\alpha^2} \frac{\partial P}{\partial z} \\ & + \frac{1}{\alpha^2} \left(\frac{1}{\zeta R} \tau_{\zeta z} + \frac{1}{R} \frac{\partial \tau_{\zeta z}}{\partial \zeta} - \frac{\partial \tau_{zz}}{\partial z} + \frac{\zeta}{R} \frac{\partial R}{\partial z} \frac{\partial \tau_{zz}}{\partial z} \right) + G_r T + G_c C - \frac{M^2}{\text{Re}} w, \end{aligned} \quad (41)$$

$$\begin{aligned} \frac{\partial T}{\partial t} = & \frac{\zeta}{R} \frac{\partial R}{\partial t} \frac{\partial T}{\partial \zeta} + \frac{\text{Re}}{\alpha^2} \left(-\frac{u}{R} \frac{\partial T}{\partial \zeta} + \frac{\zeta}{R} \frac{\partial R}{\partial z} \frac{\partial T}{\partial \zeta} w - w \frac{\partial T}{\partial \zeta} \right) \\ & + \frac{E_c}{\alpha^2} \left(\frac{\tau_{\zeta\zeta}}{R} \frac{\partial u}{\partial \zeta} + \frac{\tau_{\zeta z}}{R} \frac{\partial w}{\partial \zeta} + \tau_{\zeta z} \left[\frac{\partial u}{\partial z} - \frac{\zeta}{R} \frac{\partial R}{\partial z} \frac{\partial u}{\partial \zeta} \right] + \tau_{zz} \left[\frac{\partial w}{\partial z} - \frac{\zeta}{R} \frac{\partial R}{\partial z} \frac{\partial w}{\partial \zeta} \right] \right) \\ & + \frac{1}{\alpha^2 \text{Pr}} \left(\frac{1}{R^2} \frac{\partial^2 T}{\partial \zeta^2} + \frac{1}{\zeta R^2} \frac{\partial T}{\partial \zeta} + \frac{\partial^2 T}{\partial z^2} - \left[-\frac{\zeta}{R^2} \frac{\partial R}{\partial z} \frac{\partial T}{\partial \zeta} + \frac{\zeta}{R} \frac{\partial^2 R}{\partial z^2} \frac{\partial T}{\partial \zeta} + \frac{\zeta}{R} \frac{\partial R}{\partial z} \frac{\partial^2 T}{\partial \zeta^2} \right] \right), \end{aligned} \quad (42)$$

$$\begin{aligned} \frac{\partial C}{\partial t} = & \frac{\zeta}{R} \frac{\partial R}{\partial t} \frac{\partial C}{\partial \zeta} + \frac{\text{Re}}{\alpha^2} \left(-\frac{u}{R} \frac{\partial C}{\partial \zeta} + \frac{\zeta}{R} \frac{\partial R}{\partial z} \frac{\partial C}{\partial \zeta} w - w \frac{\partial C}{\partial \zeta} \right) \\ & + \frac{1}{\alpha^2 S_c} \left(\frac{1}{R^2} \frac{\partial^2 C}{\partial \zeta^2} + \frac{1}{\zeta R^2} \frac{\partial C}{\partial \zeta} + \frac{\partial^2 C}{\partial z^2} - \left[-\frac{\zeta}{R^2} \frac{\partial R}{\partial z} \frac{\partial C}{\partial \zeta} + \frac{\zeta}{R} \frac{\partial^2 R}{\partial z^2} \frac{\partial C}{\partial \zeta} + \frac{\zeta}{R} \frac{\partial R}{\partial z} \frac{\partial^2 C}{\partial \zeta^2} \right] \right) \\ & + \frac{S_r}{\alpha^2} \left(\frac{1}{R^2} \frac{\partial^2 T}{\partial \zeta^2} + \frac{1}{\zeta R^2} \frac{\partial T}{\partial \zeta} + \frac{\partial^2 T}{\partial z^2} - \left[-\frac{\zeta}{R^2} \frac{\partial R}{\partial z} \frac{\partial T}{\partial \zeta} + \frac{\zeta}{R} \frac{\partial^2 R}{\partial z^2} \frac{\partial T}{\partial \zeta} + \frac{\zeta}{R} \frac{\partial R}{\partial z} \frac{\partial^2 T}{\partial \zeta^2} \right] \right), \end{aligned} \quad (43)$$

Where the components of stress are defined as [59]

$$\tau_{zz} = 2\eta(\gamma) \left(\frac{\partial w}{\partial z} - \frac{\zeta}{R} \frac{\partial R}{\partial z} \frac{\partial w}{\partial \zeta} \right), \tau_{\zeta\zeta} = 2\eta(\gamma) \left(\frac{1}{R} \frac{\partial u}{\partial \zeta} \right), \tau_{\zeta z} = \eta(\gamma) \left(\frac{\partial u}{\partial z} - \frac{\zeta}{R} \frac{\partial R}{\partial z} \frac{\partial u}{\partial \zeta} + \frac{1}{R} \frac{\partial w}{\partial \zeta} \right);$$

$$\eta(\gamma) = \frac{\tau_0 + l^* \gamma^{1/2} + \gamma}{\gamma}; \quad l^* = \frac{\eta_2}{\eta_1} \left(\frac{d_0}{u_0} \right)^{1/2} \quad \text{and}$$

$$\gamma = 2 \left[\left(\frac{1}{R} \frac{\partial u}{\partial \zeta} \right)^2 + \left(\frac{u}{\zeta R} \right)^2 + \left(\frac{\partial w}{\partial z} - \frac{\zeta}{R} \frac{\partial R}{\partial z} \frac{\partial w}{\partial \zeta} \right)^2 \right] + \left(\frac{\partial u}{\partial z} - \frac{\zeta}{R} \frac{\partial R}{\partial z} \frac{\partial u}{\partial \zeta} + \frac{1}{R} \frac{\partial w}{\partial \zeta} \right)^2.$$

The radial velocity can be found as [59]

$$u(\zeta, z, t) = \zeta \left(\frac{\partial R}{\partial z} w + \frac{\partial R}{\partial t} [2 - \zeta^2] \right). \quad (44)$$

The initial conditions can be defined as:

$$w(\zeta, z, 0) = \left(\frac{A_0 + A_1}{4} \right) \left(1 - \left[\frac{\zeta R}{d_0} \right]^2 \right), \quad \text{in the absence of a magnetic field,} \quad (45a)$$

$$w(\zeta, z, 0) = \left(\frac{A_0 + A_1}{M^2} \right) \left(1 - \left[\frac{I_0(\zeta RM)}{I_0(M)} \right]^2 \right), \quad \text{in the presence of a magnetic field,} \tag{45b}$$

$$T(\zeta, z, 0) = 0, u(\zeta, z, 0) = 0, C(\zeta, z, 0) = 0. \tag{45c}$$

And the conditions of the boundary are:

$$\frac{\partial w}{\partial \zeta}(\zeta, z, t) = 0, u(\zeta, z, t) = 0, \frac{\partial C}{\partial \zeta}(\zeta, z, t) = 0, \frac{\partial T}{\partial \zeta}(\zeta, z, t) = 0 \quad \text{at } \zeta = 0, \tag{46a}$$

$$w(\zeta, z, t) = 0, u(\zeta, z, t) = \frac{\partial R}{\partial t}, C(\zeta, z, t) = 0, T(\zeta, z, t) = 0 \quad \text{at } \zeta = 1. \tag{46b}$$

5. Application of AGHPM

To apply the AGHPM algorithm to the governing Equations (41-43), in the firstly, we transform Equations (41-43) to ordinary differential equations this can be made by taking Laplace transform with respect to ζ with apply the condition on it then we have also partial differential equation in z, t coordinate and to make the equations full ordinary after that we take Yang transform with respect to z , and by applying the conditions on it, then, we have the following new system:

$$\left. \begin{aligned} w_t^* &= \frac{R_t^* \delta}{s^2 R^*} + \frac{\text{Re}}{\alpha^2} \left(-\frac{u^* \delta}{R^*} + \frac{\delta w^* \lambda}{s^2 R^*} - w^* \delta \right) - \frac{1}{\alpha^2} P_z + \frac{1}{\alpha^2} \left(\frac{s^2}{R^*} \tau_{\zeta z}^* + \frac{s}{R^*} \tau_{\zeta z}^* - \frac{1}{\beta} \tau_{zz}^* + \frac{\lambda}{s^2 R^*} \left(\frac{1}{\beta} \tau_{zz}^* \right) \right) \\ &+ G_r T^* + G_c C^* - \frac{M^2}{\text{Re}} w^*, \\ T_t^* &= \frac{R_t^* (sT^*)}{s^2 R^*} + \frac{\text{Re}}{\alpha^2} \left(-\frac{u^* (sT^*)}{R^*} + \frac{\lambda (sT^*) w^*}{s^2 R^*} - w^* (sT^*) \right) + \frac{E_c}{\alpha^2} \left(\frac{\tau_{\zeta \zeta}^* (su^*)}{R^*} + \frac{\delta \tau_{\zeta z}^*}{R^*} + \left(-\frac{\lambda (su^*)}{s^2 R^*} + \left(\frac{1}{\beta} u^* \right) \right) \tau_{\zeta z}^* \right) \\ &+ \frac{E_c}{\alpha^2} \left(\tau_{zz}^* \left(\left(\frac{1}{\beta} w^* \right) - \frac{\delta \lambda}{s^2 R^*} \right) \right) + \frac{1}{\alpha^2} \text{Pr} \left(\frac{s^2 T^*}{R^*} + \frac{s^2 (sT^*)}{R^*} + \left(\frac{T^*}{\beta^2} \right) - \left(-\frac{\lambda (sT^*)}{s^2 R^*} + \frac{(sT^*)}{s^2 R^*} \left(\frac{1}{\beta^2} R^* \right) + \frac{\lambda (s^2 T^*)}{s^2 R^*} \right) \right), \\ C_t^* &= \frac{R_t^* (sC^*)}{s^2 R^*} + \frac{\text{Re}}{\alpha^2} \left(-\frac{u^* (sC^*)}{R^*} + \frac{\lambda (sC^*) w^*}{s^2 R^*} - w^* (sC^*) \right) + \frac{1}{\alpha^2 S_c} \left(\frac{(sC^*)}{R^*} + \frac{s^2 (sC^*)}{R^*} + \frac{C^*}{\beta^2} \right) \\ &+ \frac{1}{\alpha^2 S_c} \left(-\left(\frac{\lambda (s^2 C^*)}{s^2 R^*} \right) - \left(-\frac{\lambda (sC^*)}{s^2 R^*} + \frac{(sC^*)}{s^2 R^*} \left(\frac{1}{\beta^2} R^* \right) \right) \right) + \frac{S_r}{\alpha^2} \left(\frac{(s^2 T^*)}{R^*} + \frac{s^2 (sT^*)}{R^*} + \left(\frac{T^*}{\beta^2} \right) \right) \\ &+ \frac{S_r}{\alpha^2} \left(-\left(-\frac{\lambda (sT^*)}{s^2 R^*} + \frac{(sT^*)}{s^2 R^*} \left(\frac{1}{\beta^2} R^* \right) + \frac{\lambda (s^2 T^*)}{s^2 R^*} \right) \right), \end{aligned} \right\} \tag{47}$$

where; $w^* = w^*(s, \beta, t), T^* = T^*(s, \beta, t), C^* = C^*(s, \beta, t), \delta = s w^*, \lambda = \frac{1}{\beta} R^*, \tau_{\zeta z}^* = \eta(\gamma^*) \left(\frac{u^*}{\beta} - \frac{\lambda (su^*)}{s^2 R^*} + \frac{\delta}{R^*} \right)$

$$\tau_{zz}^* = 2\eta(\gamma^*) \left(\frac{1}{\beta} w^* - \frac{\lambda (su^*)}{s^2 R^*} \right), \tau_{\zeta \zeta}^* = 2\eta(\gamma^*) \left(\frac{(su^*)}{R^*} \right) \text{ and } \eta(\gamma^*) = \frac{\tau_0 + l^* \gamma^{*1/2} + \gamma^*}{\gamma^*}; l^* = \frac{\eta_2}{\eta_1} \left(\frac{d_0}{u_0} \right)^{1/2}$$

where; $\gamma^* = \left\{ 2 \left[\left(\frac{1}{R^*} (su^*) \right)^2 + \left(\frac{s^2 u^*}{R^*} \right)^2 + \left(\frac{1}{\beta} w^* - \frac{\lambda \delta}{s^2 R^*} \right)^2 \right] + \left(\frac{1}{\beta} u^* - \frac{\lambda (su^*)}{s^2 R^*} + \frac{\delta}{R^*} \right)^2 \right\}^{1/2}$.

Also; the geometric of stenosis is:

$$R^*(\beta, t) = \begin{cases} \left(\left[m\beta^2 + d_0 \right] - \frac{\tau_m \cos(\psi)(\beta^2 - d)}{l_0} \zeta \right) a_1(t), & d \leq \beta \leq d + \frac{3}{2}l_0, \\ \left[m\beta^2 + d_0 \right] a_1(t), & \text{otherwise,} \end{cases}$$

where: $R^* = R^*(\beta, t)$, $\zeta = 11 - \frac{94(\beta^2 - d)}{3l_0} + \frac{32(\beta^2 - d)^2}{l_0^2} - \frac{32(\beta^2 - d)^3}{3l_0^3}$ and $a_1(t) = 1 + k \cos(\omega t - \phi)$.

Now, we will use the innovative algorithm AGHPM that we illustrated it in subsection (2.3) to solve the equations involved in relation (47). After finding the AGHPM solutions $w^*(s, \beta, t)$, $T^*(s, \beta, t)$, and $C^* = C^*(s, \beta, t)$, we take the Laplace and Yang inverse for these solutions to obtain: $w(t, \zeta, z)$, $T(t, \zeta, z)$ and $C(t, \zeta, z)$.

These analytical approximate solutions will be in two cases: The first in the absence of a magnetic field are;

$$\begin{aligned} w &= (a_1)(b_1) - t \left(\mathcal{G} \left[G_c \left(\mathcal{G} \left[\frac{S_r(\mathcal{G}^*(a_{11})) \left(\frac{1}{z^{-1}} \right)}{\alpha^2} \right] + G_r(\mathcal{G}^* a_{11}) + \dots \right) \right] + t^2 \left(\frac{1}{2}(\mathcal{G}^*) \left[G_c \left(\text{Re}(\mathcal{G}^*) \left[\frac{S_r(\mathcal{G}^*(a_{11})) \left(\frac{1}{z^{-1}} \right)}{\alpha^2} \right] \left[2\zeta^{-1}(b_{11}) - \frac{(2b_{11})}{z^{-1}} \right] + \dots \right) \right] \right) \right. \\ &+ t^2 \left(\frac{\mathcal{G}^*}{2} \left[\frac{G_r \left(\text{Re}(\mathcal{G}^* a_{11}) \left[2\zeta^{-1}(b_{11}) - 2 \left(\frac{1}{z^{-1}\zeta^{-1}} \right) (b_{11}) \right] \right)}{\alpha^2} \right] + \frac{A_1\omega}{\alpha^2} - \frac{\zeta^{-2}(b_{11}^*)}{\alpha^2 R^2} + \frac{4\zeta^{-1}(b_{11})}{\alpha^2 R^3} \frac{\partial R}{\partial t} + \dots \right) \Bigg) \\ T &= t(\mathcal{G}^* a_{11} + \dots) + t^2 \left(\frac{1}{2} \left[\frac{\text{Re}(\mathcal{G}^* a_{11}) \left[2\zeta^{-1}(b_{11}) - 2 \left(\frac{1}{z^{-1}\zeta^{-1}} \right) (b_{11}) \right]}{\alpha^2} + \dots \right] \right) \\ C &= t \left(\mathcal{G} \left[\frac{S_r(\mathcal{G}^*(a_{11})) \left(\frac{1}{z^{-1}} \right)}{\alpha^2} + \dots \right] + t^2 \left(\frac{1}{2} \left[\text{Re}(\mathcal{G}^*) \left[\frac{S_r(\mathcal{G}^*(a_{11})) \left(\frac{1}{z^{-1}} \right)}{\alpha^2} \right] \left[2\zeta^{-1}(b_{11}) - \frac{(2b_{11})}{z^{-1}} \right] + \dots \right] \right) \right) \end{aligned}$$

where: $a_1 = \left(\frac{A_0 + A_1}{4} \right)$, $b_1 = \left(1 - \left[\frac{\zeta R}{d_0} \right]^2 \right)$, $\mathcal{G}^* = \frac{R}{\partial R}$, $a_{11} = \frac{4E_c \zeta R^2 (a_1)^2 (-b_1)^2}{z^{-1}\alpha^2 R^2}$, $b_{11} = \frac{R \left(\frac{A_0 + A_1}{2} \right) \frac{\partial R}{\partial t}}{d_0^2 \frac{\zeta^{-3}}{6}}$, $b_{11}^* = \frac{R(A_0 + A_1) \frac{\partial R}{\partial t}}{d_0^2 \frac{\zeta^{-3}}{6}}$

Secondly, the analytical solutions in the presence of a magnetic field are:

$$\begin{aligned} w &= (a_1^*)(1 - [b_1^*]^2) + t \left(\mathcal{G}^* \left[G_c \left(\left[\frac{\alpha^2 z S_c R}{z^2 - R + \alpha^2 z S_c} \frac{\partial R}{\partial t} \right] \left[\frac{S_r(\mathcal{G}^* a_{11}^*) \left(\frac{1}{z^{-1}R} \right)}{\alpha^2} \right] + G_r(\mathcal{G}^* a_{11}^*) + \dots \right) \right] \right. \\ &+ t^2 \left(\frac{1}{2}(\mathcal{G}^*) \left(-\frac{A_1\omega}{\alpha^2} - \frac{\text{Re} \left(\zeta^{-1} b_{11}^{*2} - \frac{b_{11}^*}{z^{-1}} - \frac{2([b_1^*] - 1)(A_0 + A_1)b_{111}^*}{M^2 z^{-1}} \right)}{\alpha^2} + \dots \right) \right) \Bigg) \\ T &= t(\mathcal{G}^* a_{11}^* + \dots) + t^2 \left(\frac{1}{2}(\mathcal{G}^*) \left[\frac{\text{Re} \left(2\mathcal{G}^* a_{11}^* \right) \left[a_{11}^* [b_1^* - 1] \right]}{\alpha^2} + \dots \right] \right) \end{aligned}$$

$$C = t \left(\left[\frac{\alpha^2 z S_c R}{z^2 - R + \alpha^2 z S_c \frac{\partial R}{\partial t}} \right] \left[\frac{S_r (g^* a_{11}^*) \left(\frac{1}{z^{-1} R} \right)}{\alpha^2} + \dots \right] + t^2 \left(\frac{1}{2} g^* \left[- \frac{S_r \left(\frac{\text{Re} (2g^* a_{11}^*) a_{11}^* [b_1^* - 1]}{\alpha^2} \right) \left(\frac{1}{z} \right)}{\alpha^2} + \dots \right] \right) \right)$$

$$\text{where: } a_1^* = \left(\frac{A_0 + A_1}{M^2} \right), \quad b_1^* = \left(\frac{I_0(\zeta R M)}{I_0(M)} \right), \quad a_{11}^* = \frac{4E_c \zeta^{-1} (A_0 + A_1) (1 - [b_1^*]^2) \left(\frac{\zeta^{-1} I_1(\zeta R M) (A_0 + A_1) \frac{\partial R}{\partial t}}{M \zeta^{-1} I_0(M)} \right) R^2}{M^2 z^{-1} \alpha^2 R^2},$$

$$b_{11}^* = 2 \left(\frac{I_1(\zeta R M) (A_0 + A_1) \frac{\partial R}{\partial t}}{M \zeta^{-1} I_0(M)} \right)^2, \quad b_{111}^* = \left(\frac{I_1(\zeta R M) (2A_0 + 2A_1) \frac{\partial R}{\partial t}}{M \zeta^{-1} I_0(M)} \right)$$

Now, after we have established the velocity components (radial and axial velocity), the important properties of the blood flow like the volumetric flow rate, the wall shear stress and the resistance impedance can be calculated with the help it (velocities), as follows, respectively:

$$Q = 2\pi R^2 \int_0^1 \zeta w d\zeta, \tag{48a}$$

$$\tau = \frac{1}{R} \left(\frac{\partial w}{\partial \zeta} \right)^h \times \left\{ \cos \left(a \tan \left[\frac{dR}{\partial z} \right] \right) \right\}^h, \tag{48b}$$

$$\Lambda = \frac{\left| L \left(\frac{\partial P}{\partial z} \right) \right|}{Q}. \tag{48c}$$

6. Results and discussion

Fig. 2 shows the comparison between the analytical approximate solution offered by the new method (AGHPM) and [71] for the axial velocity in the state of the absence of a magnetic field at $A_1 = 0.2, t = 0.2, d_0 = 1, \tau_0 = 1, l^* = 4, l_0 = 7, d = 10, k = 0.005, f = 1.2, \omega = 2\pi f, S_c = 3, S_r = 3, E_c = 0.4, z = 1, \text{Re} = 1000, \alpha^2 = 2000, G_c = 1.5, G_r = 1.5$ and various values of τ_m, ψ and A_0 . While Fig. 3 explains the effect of a magnetic field on the axial velocity (presence of M) at the same values of the parameters for Fig. 2. We note that the velocity flow of blood amounts to the maximum value in the center of the artery. Moreover, it can be observed that the velocity increase as the depth of the stenosis increases (τ_m), whilst when the angle of the tapered vessel increases (ψ) the velocity decreases. Furthermore, we note the effect of a magnetic field on the velocity: when the magnetic parameter (M) increases, the velocity will decrease. This happens due to the fact that blood contains magnetic iron oxide, and when a magnetic field impacts the blood, it feels a powerful electromotive power, which leads to the generation of a rotational movement of blood particles, and these impacts the speed of blood flow. Therefore, when the influence of the magnetic field increases, the Lorenz force which is stable amongst the applied magnetic field and the magnetic particles oppose the movement of the flow of blood and thus leads the blood velocity to decrease. Consequently, we can conclude the great significance in the blood vessel when the stenosis is reduced and the magnetic field increases, because the vessels slowly dredge the blood velocity and as a result minimize the risk of disease.

Fig. 4 explains the comparison between AGHPM and Ref. [59] solutions for the effect of the solutal Grashof

number (G_c) and the Grashof number (G_r) on the axial velocity when the depth of the stenosis takes a fixed value ($\tau_m = 0.3d_0$) and $A_1 = 0.2, t = 0.2, d_0 = 1, \tau_0 = 1, l^* = 4, l_0 = 7, d = 10, k = 0.005, f = 1.2, \omega = 2\pi f, S_c = 3, S_r = 3, E_c = 0.4, \text{Re} = 1000, \alpha^2 = 2000$ and $z = 1$, in a state of absence of a magnetic field. However, Fig. 5 illustrates the impact of a magnetic parameter as well as the influence of G_c and G_r on the axial velocity (presence of M), in the same values of the parameters in Fig. 4. We show, when G_c and G_r increase the velocity also increases, which exemplifies the influence of both mass and heat on the fluid, respectively. Also, we note that when M increases, the velocity decreases. This signifies that the velocity increases considerably when the concentration and temperature growing in the absence of a magnetic field. Conversely the velocity decreases in the presence of a magnetic field which illustrate that M has an opposite effect with G_r and G_c on velocity. This occurs due to the Lorentz force which dissents the movement of the flow of blood at the artery causing an increase in blood's internal viscosity. This indicates the importance of a magnetic field in reducing the risk of diseases, when used appropriately.

Fig. 6 demonstrates the volumetric flow rate in an artery with stenosis at various values of G_r, ψ, A_0 and $d_0 = 1, \tau_0 = 1, l^* = 4, l_0 = 7, d = 10, k = 0.005, f = 1.2, \omega = 2\pi f, S_c = 3, S_r = 3, E_c = 0.4, G_c = 1.5, \text{Re} = 1000, \alpha^2 = 2000, A_1 = 0.2, t = 0.2, \tau_m = 0.4d_0$ in the absence of a magnetic field. We can observe that the volume flow rate takes the shape of the geometric artery, illustrating that the rate of flow goes down at the onset of stenosis and at the critical height of the stenosis reaches its minimum. Moreover, when ψ increases, the flow rate increases significantly. Also, the flow rate increases when the thermodynamics parameter (G_r) increases. To the contrary, as shown in Fig. 7, in the case of the flow rate with the impact of a magnetic field on its (M presence), we note that the rate of flow decreases as M increases. This means that the existence of a magnetic field also affects the rate of flow by considerably minimizing its size, also it is illustrated that M has an opposite effect with G_r on flow rate. Furthermore, Fig. 8 illustrates the comparison between AGHPM and Ref. [59] solutions for the volumetric flow rate for various values of G_c which demonstrate the influence of mass transfer on the fluid flow. It was noted that the rate of flow is subject to increases when the solutal Grashof number (G_c) increases. Conversely, Fig. 9 shows the impact of a magnetic field on the flow rate (presence of M) with various values of mass transfer represented by a G_c number. It can be seen that the rate of flow decreases with the increase in M which means that M has the opposite effect with G_c on flow rate. Due the behavior of blood as an electrically conductive fluid that stimulates the magnetic field as well as the electric field when it flows under the effect of the magnetic field this leads to appear the Lorentz force, which opposes the movement of blood flow.

Figs. 10 and 11 explain the effect of the Grashof and solutal Grashof numbers on the wall shear stress at some tapered angles in the absence of a magnetic field and $\alpha^2 = 2000, \text{Re} = 1000, d_0 = 1, \tau_0 = 1, l^* = 4, l_0 = 7, d = 10, k = 0.005, f = 1.2, \omega = 2\pi f, S_c = 3, S_r = 3, t = 0.2, A_1 = 0.2, E_c = 0.4$. It was noted that when $\psi < 0$ the wall shear tapering converged, and if $\psi = 0$ the wall shear became a non-tapered artery. When $\psi > 0$, the wall shear tapering diverged. Moreover, at an increased solutal Grashof number and Grashof number the wall shear stress decreased greatly, i.e. the concentration and temperature exerted a negative impact on the wall shear stress. Figs. 12 and 13, however, show the effect of a magnetic field in addition to the effect of a Grashof number and solutal Grashof number on the wall shear stress (presence of M) in a range of tapered angles and with the same values of parameters in Figs. 10 and 11. It can be noticed that the wall shear stress increased with increases in the magnetic field, the Grashof number and the solute Grashof number, meaning that the temperature and concentration together with the effect of a magnetic field have a positive influence on the wall shear stress.

The effect of the Grashof number and the solute Grashof number on the flow resistance can be seen in Figs. 14 and 15 respectively; for some values of angles of tapering and $\text{Re} = 1000, \alpha^2 = 2000, d_0 = 1, \tau_0 = 1, l^* = 4, l_0 = 7, d = 10, k = 0.005, f = 1.2, \omega = 2\pi f, S_c = 3, S_r = 3, E_c = 0.4, t = 0.2, A_1 = 0.2$. In Figs. 14 and 15

the resistance of blood flow is at the critical rising point of the stenosis at its maximum value. Moreover, it was noted that the shape of the resistance flow distribution takes an opposite form to that of the rate of flow. Also, it can be noticed when the angle of a tapered vessel increases the resistance flow decreases. When the Grashof and solutal Grashof numbers increase, the resistance flow also decreases. Conversely, Figs. 16 and 17 illustrate the impact of a magnetic field on the resistance (presence of M) of the blood flow for the same values of parameters in Figs. 14 and 15. The resistance flow was observed to increase with the increase of the magnetic parameter, which indicates that the application of the magnetic field affects the flow resistance of blood. Moreover it is noted that the magnetic parameter has an opposite effect with the Grashof and solutal Grashof numbers on the flow resistance.

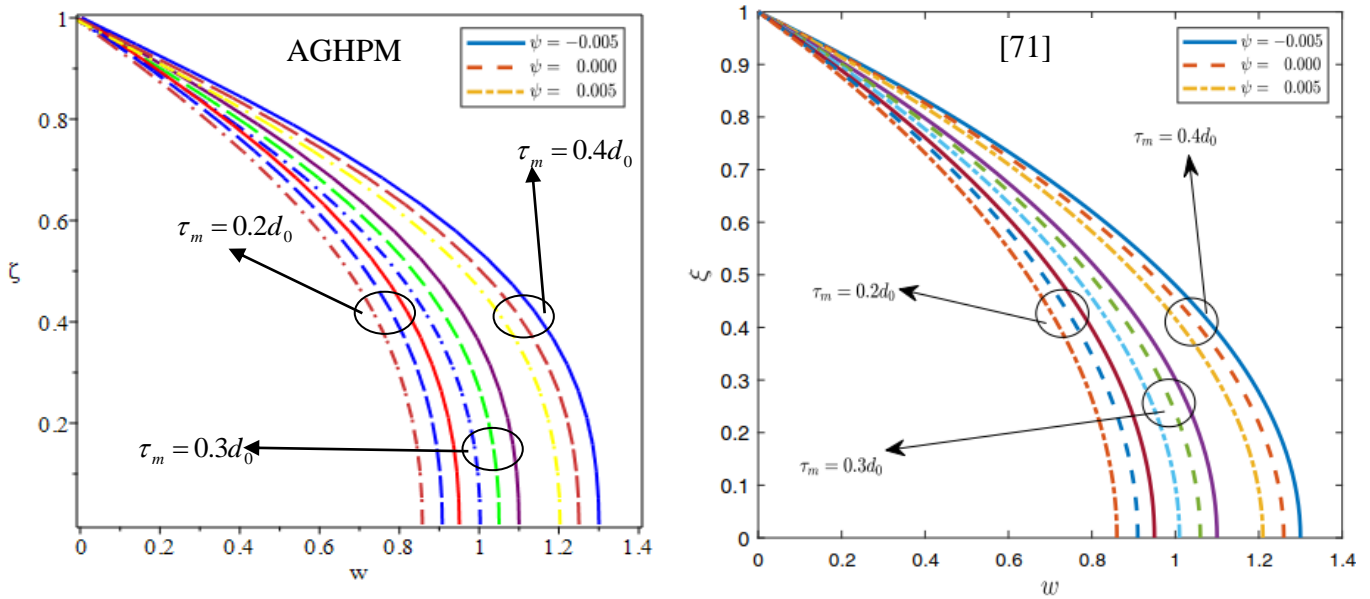


Fig. 2: Comparison between AGHPM and [71] of the axial velocity at various value of τ_m and ψ .

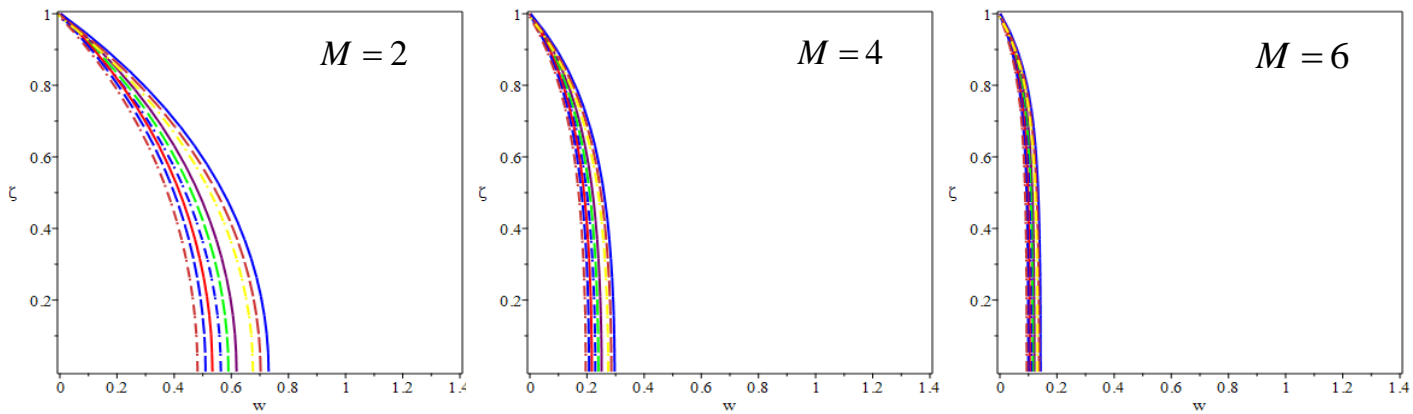


Fig. 3: Impact of magnetic field on axial velocity (w) at various value of M .

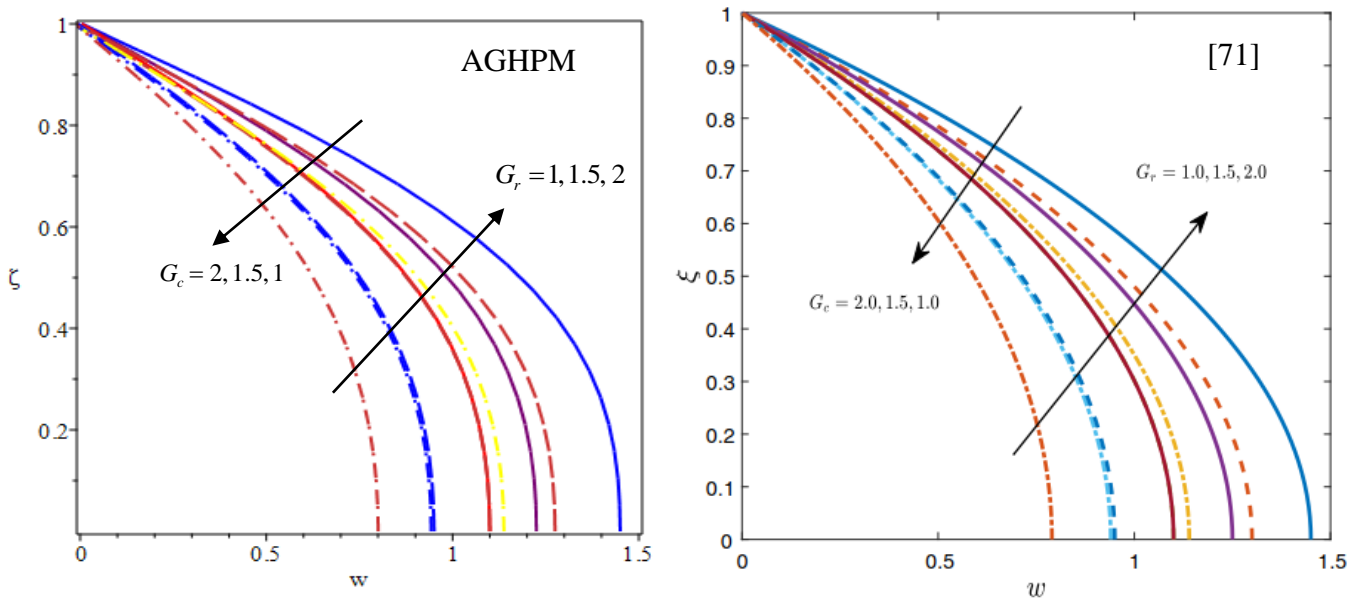


Fig. 4: Comparison between AGHPM and [71] at various value of G_r , G_c and ψ .

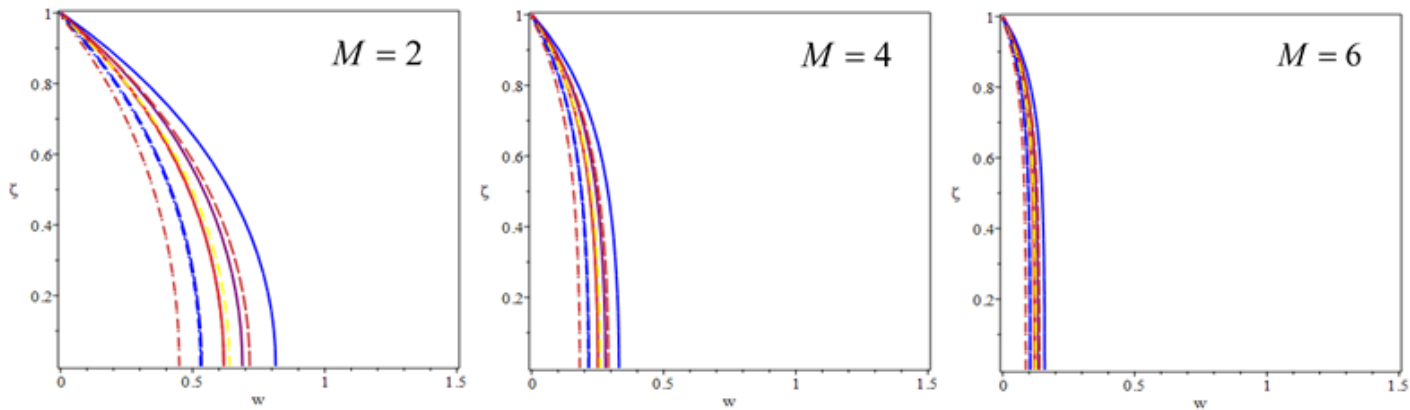


Fig. 5: Impact of magnetic field on axial velocity (w) at various value of M .

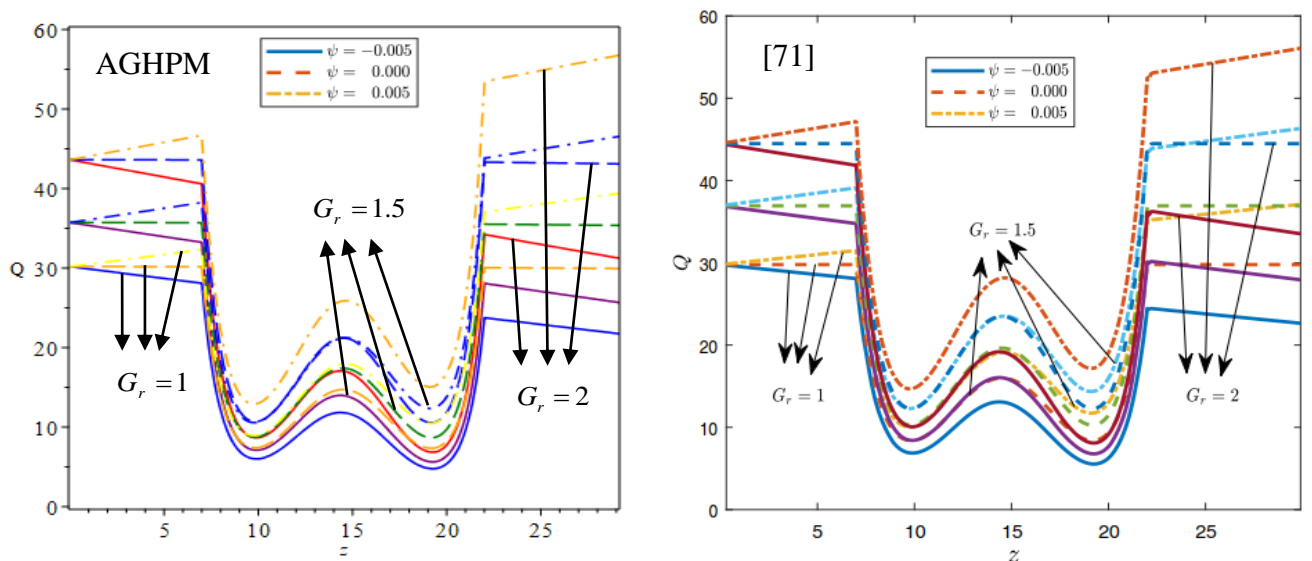


Fig. 6: Flow rate (Q) comparison between AGHPM and [71] at different values of G_r and ψ .

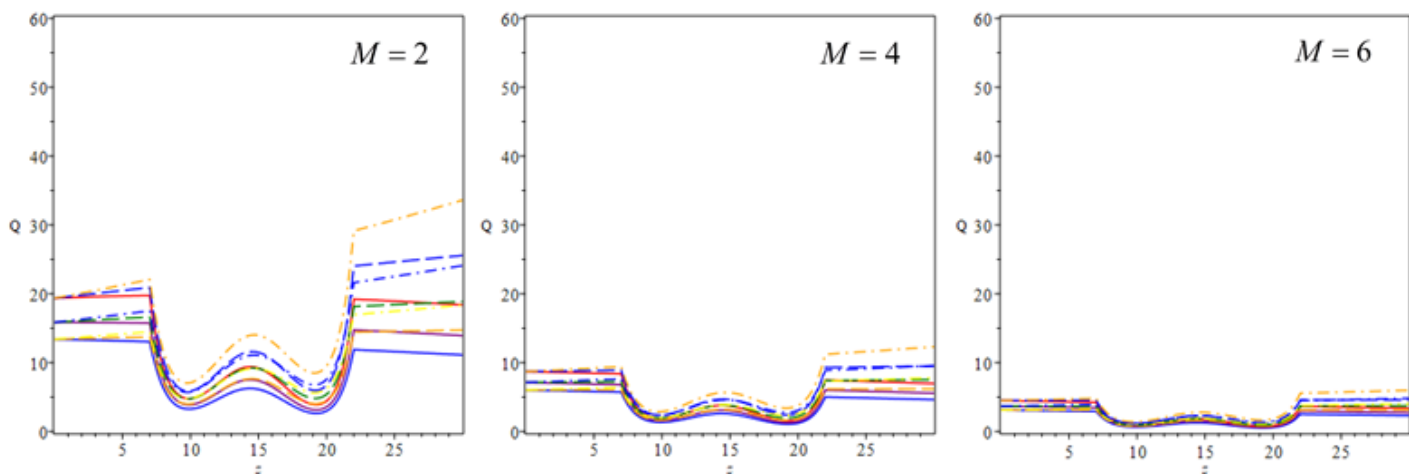


Fig. 7: Impact of magnetic field on flow rate (Q) at various values of G_r and M .

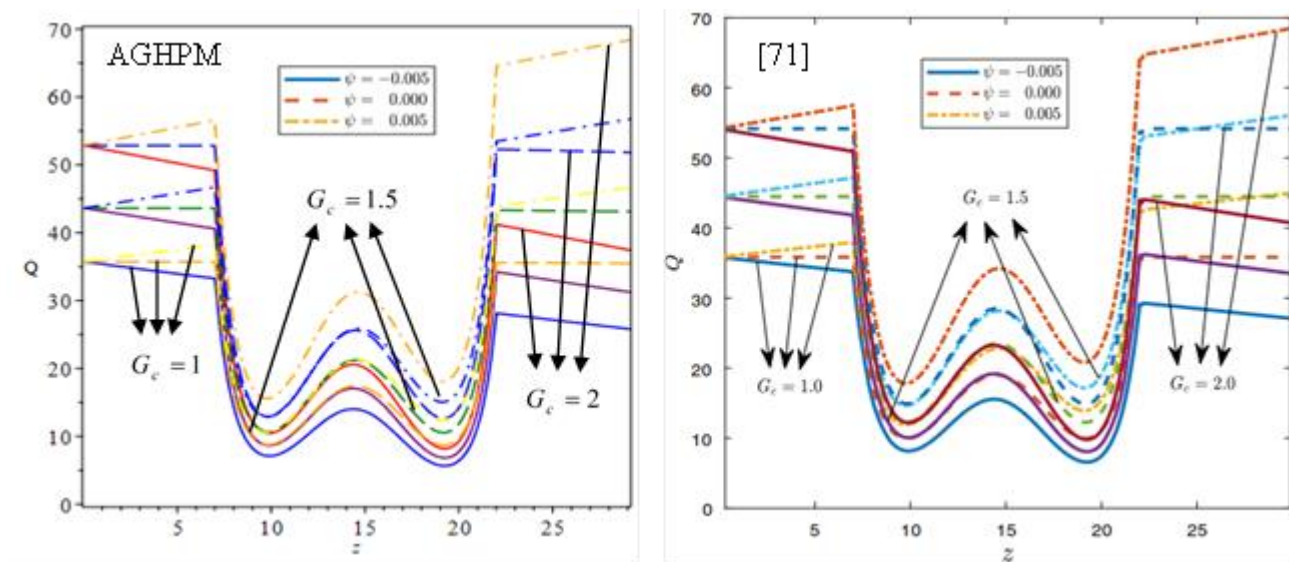


Fig. 8: Flow rate (Q) comparison between AGHPM and [71] at different values of G_c and ψ .

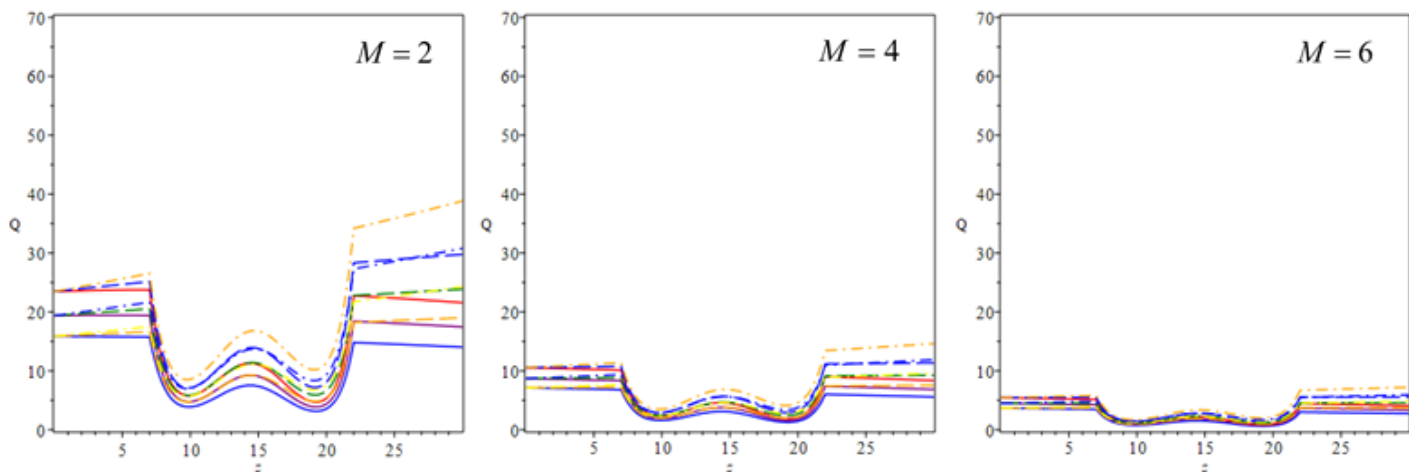


Fig. 9: Impact of magnetic field on flow rate (Q) at various values of G_c and M .

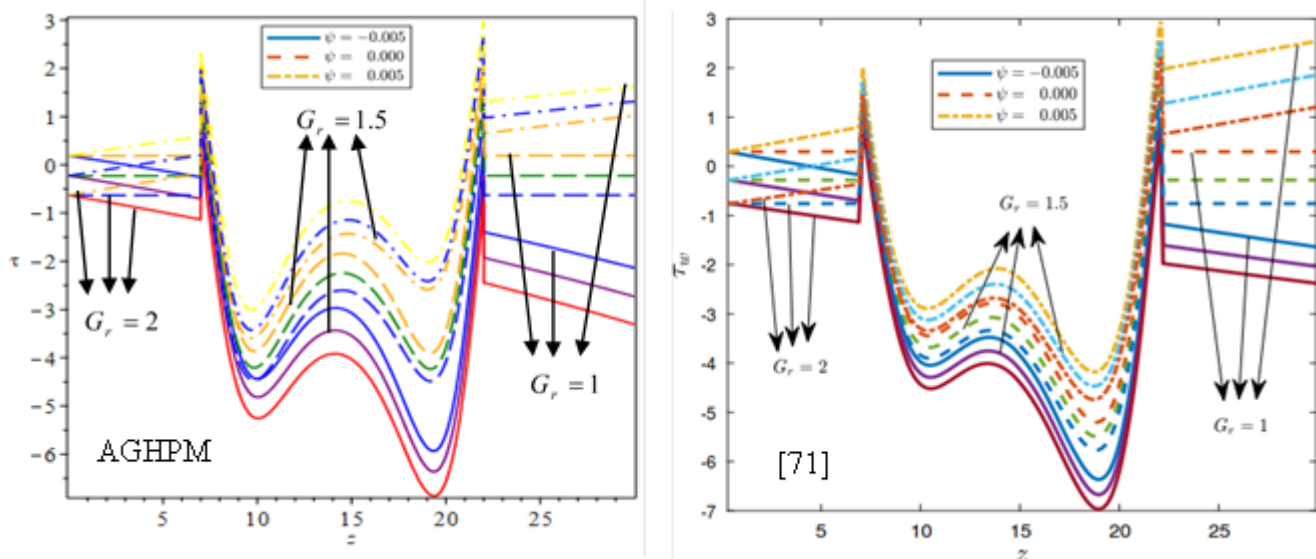


Fig. 10: AGHPM and [71] for wall shear stress (τ) at different values of G_r and ψ .

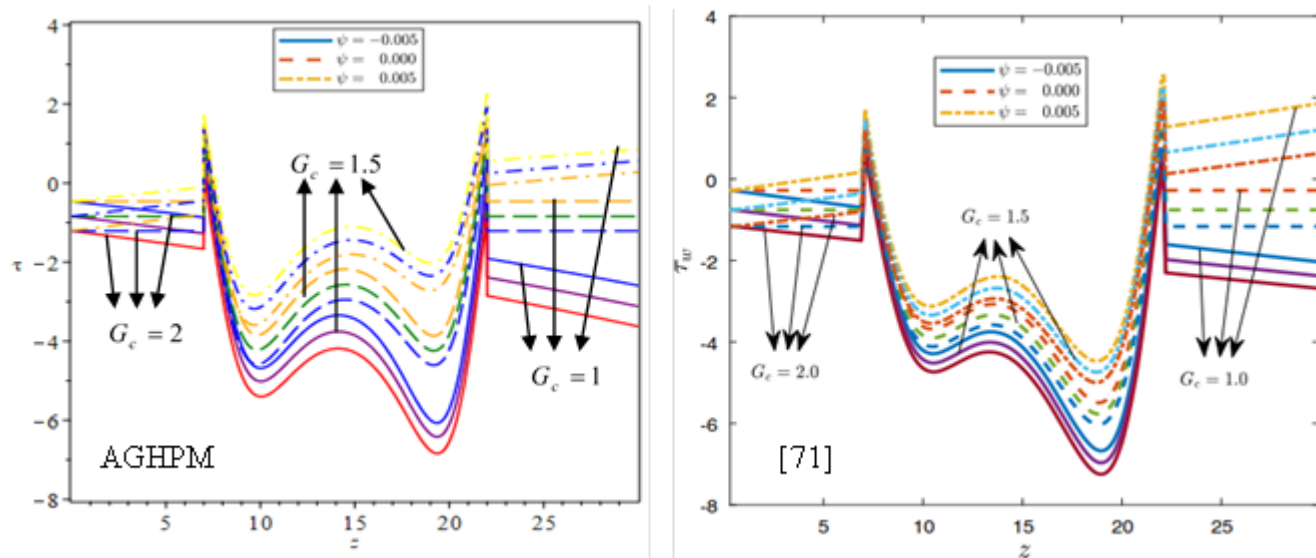


Fig. 11: AGHPM and [71] for wall shear stress (τ) at different values of G_c and ψ .

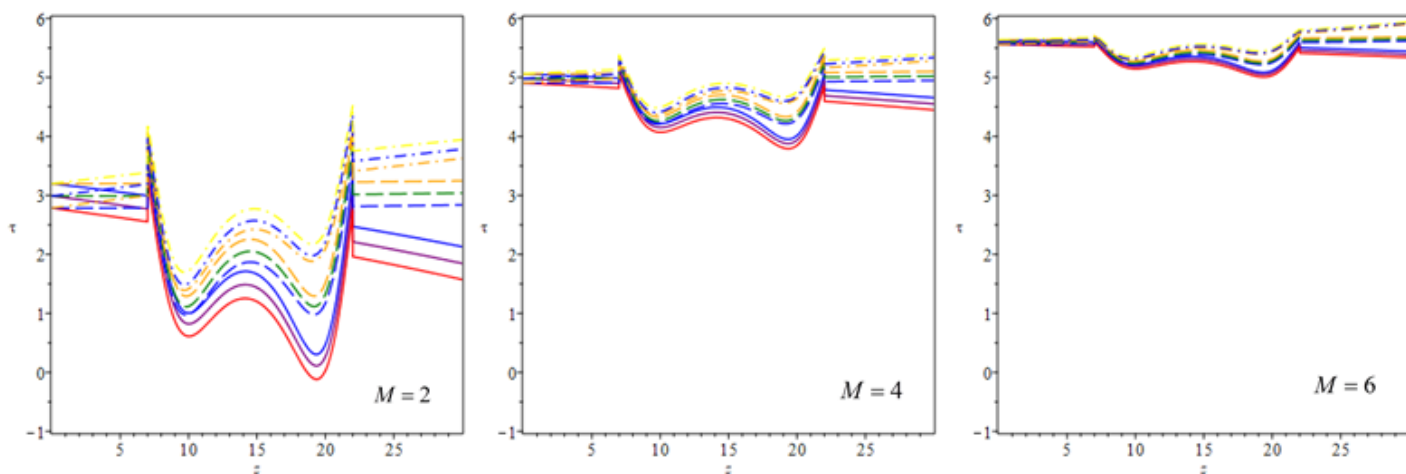


Fig. 12: The impact of magnetic field on wall shear stress (τ) at different values of G_r and $M = 2,4,6$.

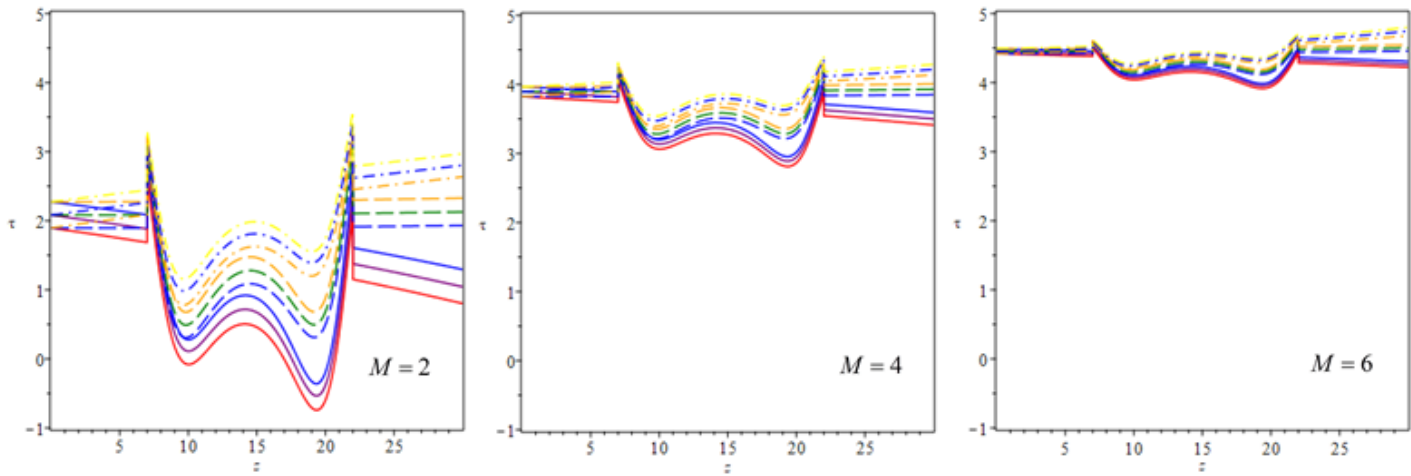


Fig. 13: The impact of magnetic field on wall shear stress (τ) at different values of G_c and $M = 2,4,6$.

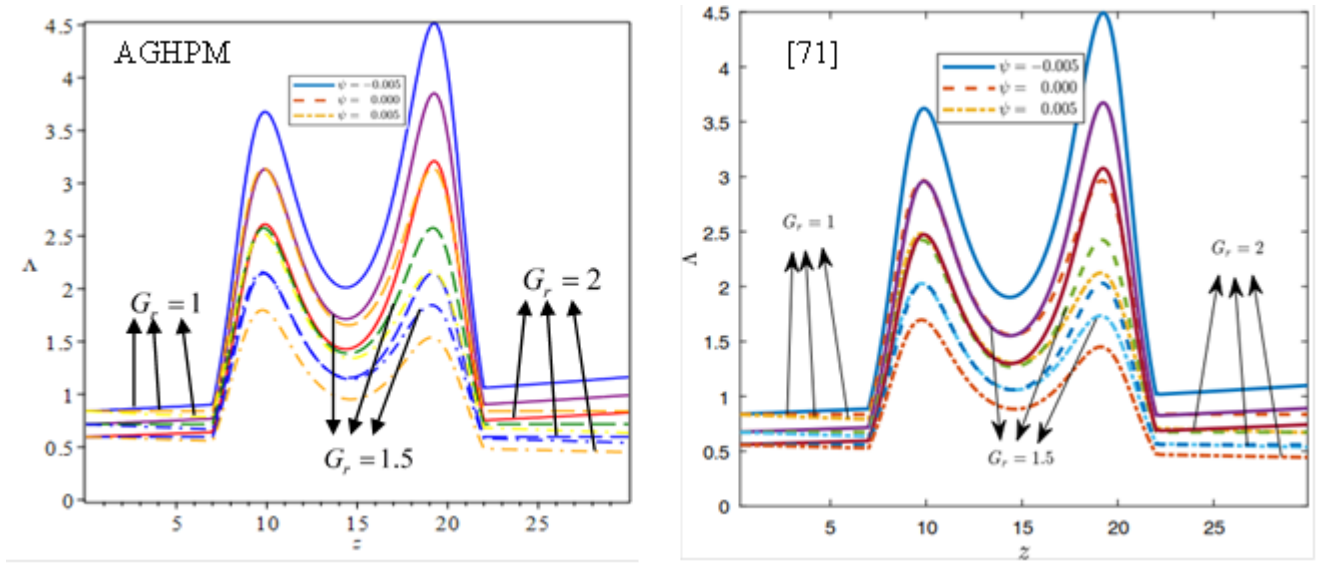


Fig. 14: The flow resistance (Λ) for AGHPM and [71] at different values of G_r and ψ .

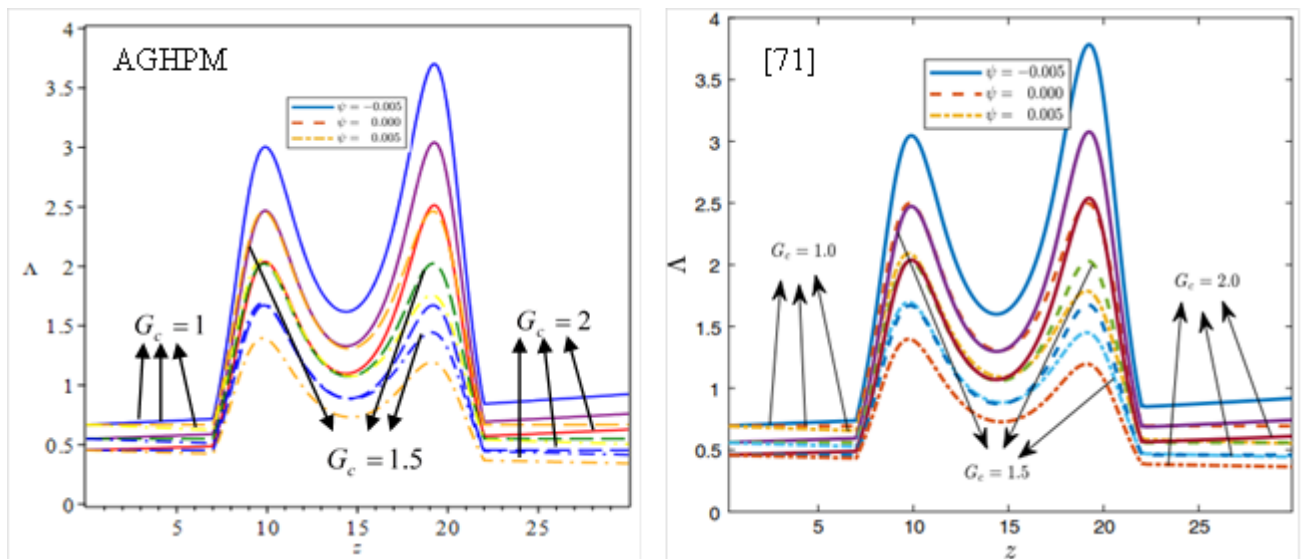


Fig. 15: The flow resistance (Λ) for AGHPM and [71] at different values of G_c and ψ .

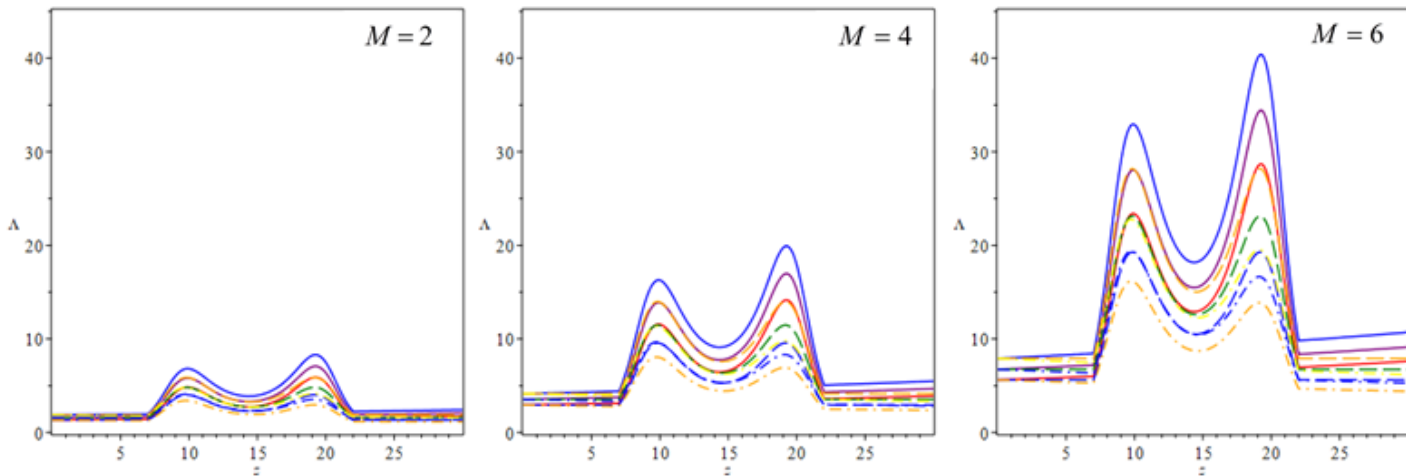


Fig. 16: Effect of magnetic field on flow resistance (Λ) at various values of G_r and $M = 2,4,6$.

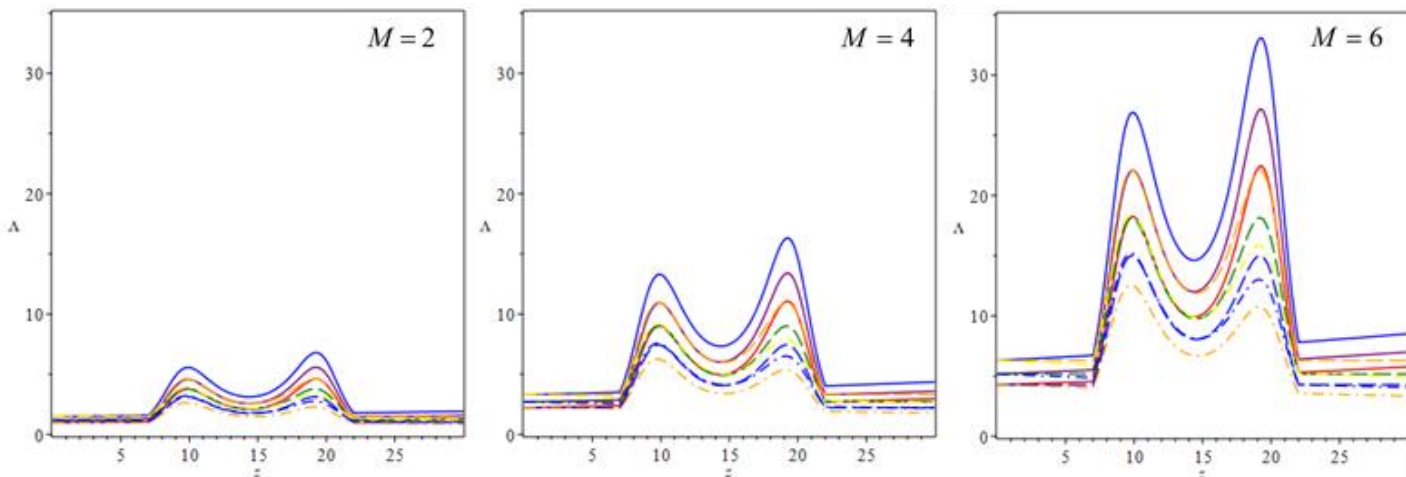


Fig. 17: Effect of magnetic field on flow resistance (Λ) at various values of G_c and $M = 2,4,6$.

Moreover; Table 1 shows the comparison of the errors between AGHPM, AGM and HPM in case of absence and presence of a magnetic field at $A_1 = 0.2, t = 0.2, d_0 = 1, \tau_0 = 1, l^* = 4, l_0 = 7, d = 10, k = 0.005, f = 1.2, \omega = 2\pi f, S_c = 3, S_r = 3, z = 1, E_c = 0.4, Re = 1000, \alpha^2 = 2000$ and different values of ψ . As shown in the tables below, AGHPM has fewer errors, is more efficient, and is more accurate than other approaches for solving this problem (AGM and HPM). As a result, we can state that the new approach is a step forward for AGM and HPM (which is the first time that we applied these methods (HPM and AGM) for solve the current problem).

Table 1: A comparison errors between AGHPM, AGM and HPM of velocity function.

ψ	Errors	$M = 0$			$M = 2$		
		AGHPM	AGM	HPM	AGHPM	AGM	HPM
-0.005	L_2	0.0000291	0.0886898	0.0217303	0.0001824	0.0441785	0.0073814
	L_∞	0.0000434	0.1988725	0.0637615	0.0006429	0.0873843	0.0251249
0	L_2	0.0000289	0.0885481	0.0217189	0.0001811	0.0440930	0.0073783
	L_∞	0.0000432	0.1989316	0.0637496	0.0006439	0.0873885	0.0251209
0.005	L_2	0.0000287	0.0883993	0.0217076	0.0001798	0.0440077	0.0073752
	L_∞	0.0000430	0.1989892	0.0637376	0.0006448	0.0873927	0.0251169

where; the measurement errors define as following:

$$L_2 = \sqrt{h \left(\sum_{i=0}^n (|w_{i+1}(\zeta) - w_i(\zeta)|)^2 \right)}$$

$$L_\infty = \text{Max}(|w_{i+1}(\zeta) - w_i(\zeta)|)$$

7. Convergence analysis of AGHPM

In this section, we will study the convergence of analytical approximate solution obtained from AGHPM for Equations (41-43), as follows:

Definition: Assume that X is the Banach space and $N: X \rightarrow \mathbb{R}$ is a nonlinear mapping where \mathbb{R} is the real numbers. Then, the sequence of the solutions can be written in the following form:

$$W_m = N(W_{m-1}), \quad W_{m-1} = \sum_{i=0}^{m-1} w_i, \quad m = 1, 2, 3, \dots \quad (49a)$$

where N satisfies the Lipschitz condition such that:

$$\forall \gamma \in \mathbb{R}; \quad \|N(W_m) - N(W_{m-1})\| \leq \gamma \|W_m - W_{m-1}\|, \quad 0 < \gamma < 1. \quad (49b)$$

Theorem (1): The series of analytical approximate solutions obtained by new method convergence if it satisfies the following condition:

$$\|W_m - W_n\| \rightarrow 0 \quad \text{when } n \rightarrow \infty, \quad 0 < \gamma < 1.$$

Proof:

$$\begin{aligned} \|W_m - W_n\| &= \left\| \sum_{i=0}^m w_i - \sum_{i=0}^n w_i \right\| \\ &= \left\| w_0 + \sum_{i=1}^m N(w_i^\bullet) - w_0 + \sum_{i=1}^n N(w_i^*) \right\|, \\ &= \left\| \sum_{i=1}^m N(w_i^\bullet) + \sum_{i=1}^n N(w_i^*) \right\|, \quad W_m = N(W_{m-1}) \\ &= \left\| N\left(\sum_{i=0}^{m-1} w_i^\bullet\right) + N\left(\sum_{i=0}^{n-1} w_i^*\right) \right\| \\ &\leq \gamma \|W_{m-1} - W_{n-1}\| \end{aligned}$$

Because N satisfies the Lipschitz condition,

Let, $m = n + 1$ then, we have $\|W_{n+1} - W_n\| \leq \gamma \|W_n - W_{n-1}\|$, then

$$\|W_n - W_{n-1}\| \leq \gamma \|W_{n-1} - W_{n-2}\| \leq \dots \leq \gamma^{n-1} \|W_1 - W_0\| \quad (50)$$

From (50), we have:

$$\begin{aligned} \|W_2 - W_1\| &\leq \gamma \|W_1 - W_0\| \\ \|W_3 - W_2\| &\leq \gamma^2 \|W_1 - W_0\| \\ &\vdots \\ \|W_n - W_{n-1}\| &\leq \gamma^{n-1} \|W_1 - W_0\| \end{aligned}$$

By using the triangle inequality:

$$\begin{aligned} \|W_m - W_n\| &= \|W_m - W_{m-1} - \dots - W_{n+1} - W_n\| \\ &\leq \|W_m - W_{m-1}\| + \|W_{m-1} - W_{m-2}\| + \dots + \|W_{n+1} - W_n\| \\ &\leq (\gamma^{m-1} + \gamma^{m-2} + \dots + \gamma^n) \|W_1 - W_0\| \\ &\leq \frac{\gamma^n}{1 - \gamma} \|W_1 - W_0\| \end{aligned}$$

when $n \rightarrow \infty$, we have $\|W_m - W_n\| \rightarrow 0$, then W_m is the Cauchy sequence in Banach space X_1 .

Theorem (2): The solution by the new method converges and is close to the solution of problems (41-43) if the following property is achieved:

$$\lim_{m \rightarrow \infty} N(W_m) = W_m$$

Proof: For any $W \in X_1$ define an operator from X_1 to X_1 , $\ell(W) = W_0 + N(W)$.

Let, $W_1, W_2 \in X_1$, then we have:

$$\begin{aligned} \|\ell(W_1) - \ell(W_2)\| &= \|W_0 + N(W_1) - W_0 - N(W_2)\| \\ &\leq \|N(W_1) - N(W_2)\| \\ &\leq \gamma \|W_1 - W_2\| \end{aligned}$$

Therefore, the mapping ℓ is contractive, and by the Banach fixed point theorem for contractive, there is a unique solution; $\ell(W_1) = W_1$.

Then:

$$\begin{aligned} \lim_{m \rightarrow \infty} N(W_m) &= N\left(\lim_{m \rightarrow \infty} W_m\right) \\ &= N\left(\lim_{m \rightarrow \infty} \sum_{i=0}^n w_i\right) \\ &= W_m \end{aligned}$$

This end the proof. ■

From Theorems (1) and (2), the values of the parameter γ^m must be calculated to obtain the convergence by using the following relationship:

$$\gamma^m = \begin{cases} \frac{\|W_{m+1} - W_m\|}{\|W_1 - W_0\|}, & \|W_1\| \neq 0, \|W_0\| \neq 0, \quad m = 1, 2, 3, \dots \\ 0, & \|W_1\| = 0, \|W_0\| = 0 \end{cases} \tag{51}$$

We can analyze the convergence of solutions in the two cases as follows:

In the absence of a magnetic field:

$$\|w_1 - w_0\| = \left\| -t \left[\mathcal{G}^* \left[G_c \left[\mathcal{G}^* \left[\frac{S_r(\mathcal{G}^*)(a_{11}) \left(\frac{1}{z^{-1}} \right)}{\alpha^2} \right] + G_r(\mathcal{G}^* a_{11}) + \dots \right] - \left(\left(\frac{A_0 + A_1}{4} \right) \left(1 - \left[\frac{\zeta R}{d_0} \right]^2 \right) \right) \right] \right] \right\|$$

$$\|w_2 - w_1\| \leq \|w_1 - w_0\| \gamma, \quad \gamma = 0.000003205 < 1,$$

$$\|w_3 - w_2\| \leq \|w_1 - w_0\| \gamma^2, \quad \gamma^2 = 7.9440E - 7 < 1,$$

:

$$\|w_m - w_{m-1}\| \leq \|w_1 - w_0\| \gamma^m.$$

In the presence of a magnetic field:

$$\|w_1 - w_0\| = \left\| t \left[\mathcal{G}^* \left[G_c \left[\left[\frac{\alpha^2 z S_c R}{z^2 - R + \alpha^2 z S_c \frac{\partial R}{\partial t}} \right] \left[\frac{S_r(\mathcal{G}^* a_{11}^*) \left(\frac{1}{z^{-1} R} \right)}{\alpha^2} \right] + G_r(\mathcal{G}^* a_{11}^*) + \dots \right] - \left(\left(\frac{A_0 + A_1}{M^2} \right) \left(1 - \left[\frac{I_0(\zeta R M)}{I_0(M)} \right]^2 \right) \right) \right] \right] \right\|$$

$$\|w_2 - w_1\| \leq \|w_1 - w_0\| \gamma, \quad \gamma = 8.4263E - 7 < 1,$$

$$\|w_3 - w_2\| \leq \|w_1 - w_0\| \gamma^2, \quad \gamma^2 = 3.6367E - 10 < 1,$$

:

$$\|w_m - w_{m-1}\| \leq \|w_1 - w_0\| \gamma^m.$$

From the above analysis, the condition of convergence was achieved in the cases both of the absence and the presence of a magnetic field. This confirms the effectiveness of the current method AGHPM in finding analytical approximate solutions. Also, it shows that the convergence theorems can be successfully applied.

8. Conclusion

In this study, the developed a problem for two-dimensional (2D) pulsatile blood flow in tapered stenosis arteries under the impact of a magnetic field in addition to the effect of mass and heat transfer was solved analytically by using a new method (AGHPM). The model that we developed through adding the effect of magnetic field on it explains the following results,

1. When M increases, the velocity and flow rate decrease,
2. When M increases, the wall shear stress and resistance flow increase.
3. Also it is concluded through the comparison between AGHPM, AGM and HPM, note that the solutions obtained using AGHPM in the case of absence and presence of a magnetic field are more accurate than other methods (AGM and HPM) which consider as developed method for AGM and HPM.
4. Furthermore; this study illustrates the importance of a magnetic field when applied to the blood flow to reduce the risk of diseases, when used appropriately.
5. Moreover, the results confirm the veracity and capacity of the new method to solve this problem, and by comparing it with previously published results they were found to be in excellent agreement with them.
6. It was concluded that AGHPM is an efficient method with a high level of accuracy in finding analytical approximate solutions for 2D pulsatile blood flow in tapered stenosis arteries under the impact of a magnetic field together with the effect of mass and heat transfer. It can be used to deal with different complicated fluid flow problems that have multiple applications in life.

9. Nomenclature

$\bar{R}(\bar{z}, \bar{t})$	The artery radius.
ψ	The tapering angle.
τ_m	The stenosis critical height.
\bar{d}	The stenosis location.
\bar{L}	The arterial segment finite length.
$\frac{3}{2}\bar{l}_0$	The interfered stenosis length.
ρ	The density of fluid.
\bar{u} and \bar{w}	The velocity components in radial and axial directions respectively.
\bar{C}	The mass concentration.
\bar{T}	The temperature.
k^*	The conductivity thermal.
\bar{P}	Pressure.
c_p	The specific heat at constant pressure.
D	The thermal-diffusion ratio.
K_T	The mass diffusivity coefficients.
T_m	The medium's temperature.
J	The current density.
σ	The electrical conductivity.
E	The electric field.
η_1	The viscosity of plasma.
d_0	The fixed radius of the normal artery located in the non-stenosis part.
u_0	The velocity average of flow in the uniform artery.
\bar{C}_0 and \bar{T}_0	The concentration of mass and average temperature respectively.

S_c, S_r, G_c	Schmidt, Soret, solutal Grashof numbers.
G_r, E_c, Pr	Grashof, Eckert, Prandtl numbers.
Re	Reynolds number.
I_0	The modulation Bessel function for the first type of order zero.
M	The magnetic field.

References

- [1] N. Ali, A. Zaman, M. Sajid, Unsteady blood flow through a tapered stenotic artery using Sisko model, *Computers & Fluids*, Vol. 101, pp. 42-49, 2014.
- [2] S. Chakravarty, P. Mandal, A nonlinear two-dimensional model of blood flow in an overlapping arterial stenosis subjected to body acceleration, *Mathematical and computer modelling*, Vol. 24, No. 1, pp. 43-58, 1996.
- [3] S. Changdar, S. De, Analysis of non-linear pulsatile blood flow in artery through a generalized multiple stenosis, *Arabian Journal of Mathematics*, Vol. 5, No. 1, pp. 51-61, 2016.
- [4] P. K. Mandal, S. Chakravarty, A. Mandal, N. Amin, Effect of body acceleration on unsteady pulsatile flow of non-Newtonian fluid through a stenosed artery, *Applied Mathematics and Computation*, Vol. 189, No. 1, pp. 766-779, 2007.
- [5] V. Srivastava, R. Rastogi, R. Vishnoi, A two-layered suspension blood flow through an overlapping stenosis, *Computers & Mathematics with Applications*, Vol. 60, No. 3, pp. 432-441, 2010.
- [6] A. Zaman, N. Ali, M. Sajid, T. Hayat, Effects of unsteadiness and non-Newtonian rheology on blood flow through a tapered time-variant stenotic artery, *AIP advances*, Vol. 5, No. 3, pp. 037129, 2015.
- [7] M. S. Dada, F. Alamu-Awoniran, Heat and Mass Transfer in Micropolar Model for Blood Flow Through a Stenotic Tapered Artery, *Applications and Applied Mathematics: An International Journal (AAM)*, Vol. 15, No. 2, pp. 24, 2020.
- [8] G. Shit, S. Majee, Pulsatile flow of blood and heat transfer with variable viscosity under magnetic and vibration environment, *Journal of Magnetism and Magnetic Materials*, Vol. 388, pp. 106-115, 2015.
- [9] S. Shaw, P. Murthy, S. Pradhan, The effect of body acceleration on two dimensional flow of Casson fluid through an artery with asymmetric stenosis, *The Open Conservation Biology Journal*, Vol. 2, No. 1, 2010.
- [10] M. Sharma, R. Gaur, INTERNATIONAL JOURNAL OF ENGINEERING SCIENCES & RESEARCH TECHNOLOGY MODELING OF MHD BLOOD FLOW IN A BALLOON CATHETERIZED ARTERIAL STENOSIS WITH THERMAL RADIATION.
- [11] R. Ponalagusamy, S. Priyadharshini, A numerical model on pulsatile flow of magnetic nanoparticles as drug carrier suspended in Herschel–Bulkley fluid through an arterial stenosis under external magnetic field and body force, *International Journal of Computer Mathematics*, Vol. 96, No. 9, pp. 1763-1786, 2019.
- [12] B. Tripathi, B. Sharma, Effect of variable viscosity on MHD inclined arterial blood flow with chemical reaction, *International Journal of Applied Mechanics and Engineering*, Vol. 23, No. 3, 2018.
- [13] R. Ellahi, S. Rahman, S. Nadeem, Blood flow of Jeffrey fluid in a catheterized tapered artery with the suspension of nanoparticles, *Physics Letters A*, Vol. 378, No. 40, pp. 2973-2980, 2014.
- [14] M. Danesh, A. Farajpour, M. Mohammadi, Axial vibration analysis of a tapered nanorod based on nonlocal elasticity theory and differential quadrature method, *Mechanics Research Communications*, Vol. 39, No. 1, pp. 23-27, 2012.
- [15] S. Faghiri, S. Akbari, M. B. Shafii, K. Hosseinzadeh, Hydrothermal analysis of non-Newtonian fluid flow (blood) through the circular tube under prescribed non-uniform wall heat flux, *Theoretical and Applied Mechanics Letters*, Vol. 12, No. 4, pp. 100360, 2022.
- [16] K. Hosseinzadeh, S. Salehi, M. Mardani, F. Mahmoudi, M. Waqas, D. Ganji, Investigation of nano-Bioconvective fluid motile microorganism and nanoparticle flow by considering MHD and thermal radiation, *Informatics in Medicine Unlocked*, Vol. 21, pp. 100462, 2020.

- [17] M. Mohammadi, A. Farajpour, A. Moradi, M. Hosseini, Vibration analysis of the rotating multilayer piezoelectric Timoshenko nanobeam, *Engineering Analysis with Boundary Elements*, Vol. 145, pp. 117-131, 2022.
- [18] M. Mohammadi, A. Rastgoo, Primary and secondary resonance analysis of FG/lipid nanoplate with considering porosity distribution based on a nonlinear elastic medium, *Mechanics of Advanced Materials and Structures*, Vol. 27, No. 20, pp. 1709-1730, 2020.
- [19] M. Mohammadi, M. Hosseini, M. Shishesaz, A. Hadi, A. Rastgoo, Primary and secondary resonance analysis of porous functionally graded nanobeam resting on a nonlinear foundation subjected to mechanical and electrical loads, *European Journal of Mechanics-A/Solids*, Vol. 77, pp. 103793, 2019.
- [20] M. Mohammadi, A. Rastgoo, Nonlinear vibration analysis of the viscoelastic composite nanoplate with three directionally imperfect porous FG core, *Structural Engineering and Mechanics, An Int'l Journal*, Vol. 69, No. 2, pp. 131-143, 2019.
- [21] A. Farajpour, A. Rastgoo, M. Mohammadi, Vibration, buckling and smart control of microtubules using piezoelectric nanoshells under electric voltage in thermal environment, *Physica B: Condensed Matter*, Vol. 509, pp. 100-114, 2017.
- [22] A. Farajpour, M. H. Yazdi, A. Rastgoo, M. Loghmani, M. Mohammadi, Nonlocal nonlinear plate model for large amplitude vibration of magneto-electro-elastic nanoplates, *Composite Structures*, Vol. 140, pp. 323-336, 2016.
- [23] A. Farajpour, M. Yazdi, A. Rastgoo, M. Mohammadi, A higher-order nonlocal strain gradient plate model for buckling of orthotropic nanoplates in thermal environment, *Acta Mechanica*, Vol. 227, No. 7, pp. 1849-1867, 2016.
- [24] M. Mohammadi, M. Safarabadi, A. Rastgoo, A. Farajpour, Hygro-mechanical vibration analysis of a rotating viscoelastic nanobeam embedded in a visco-Pasternak elastic medium and in a nonlinear thermal environment, *Acta Mechanica*, Vol. 227, No. 8, pp. 2207-2232, 2016.
- [25] M. R. Farajpour, A. Rastgoo, A. Farajpour, M. Mohammadi, Vibration of piezoelectric nanofilm-based electromechanical sensors via higher-order non-local strain gradient theory, *Micro & Nano Letters*, Vol. 11, No. 6, pp. 302-307, 2016.
- [26] M. Baghani, M. Mohammadi, A. Farajpour, Dynamic and stability analysis of the rotating nanobeam in a nonuniform magnetic field considering the surface energy, *International Journal of Applied Mechanics*, Vol. 8, No. 04, pp. 1650048, 2016.
- [27] M. Goodarzi, M. Mohammadi, M. Khooran, F. Saadi, Thermo-mechanical vibration analysis of FG circular and annular nanoplate based on the visco-pasternak foundation, *Journal of Solid Mechanics*, Vol. 8, No. 4, pp. 788-805, 2016.
- [28] H. Asemi, S. Asemi, A. Farajpour, M. Mohammadi, Nanoscale mass detection based on vibrating piezoelectric ultrathin films under thermo-electro-mechanical loads, *Physica E: Low-dimensional Systems and Nanostructures*, Vol. 68, pp. 112-122, 2015.
- [29] M. Safarabadi, M. Mohammadi, A. Farajpour, M. Goodarzi, Effect of surface energy on the vibration analysis of rotating nanobeam, 2015.
- [30] M. Goodarzi, M. Mohammadi, A. Gharib, Techno-Economic Analysis of Solar Energy for Cathodic Protection of Oil and Gas Buried Pipelines in Southwestern of Iran, in *Proceeding of*, [https://publications.waset.org/abstracts/33008/techno-economic-analysis-of ...](https://publications.waset.org/abstracts/33008/techno-economic-analysis-of-...), pp.
- [31] M. Mohammadi, A. A. Nekounam, M. Amiri, The vibration analysis of the composite natural gas pipelines in the nonlinear thermal and humidity environment, in *Proceeding of*, <https://civilica.com/doc/540946/>, pp.
- [32] M. Goodarzi, M. Mohammadi, M. Rezaee, Technical Feasibility Analysis of PV Water Pumping System in Khuzestan Province-Iran, in *Proceeding of*, [https://publications.waset.org/abstracts/18930/technical-feasibility ...](https://publications.waset.org/abstracts/18930/technical-feasibility-...), pp.
- [33] M. Mohammadi, A. Farajpour, A. Moradi, M. Ghayour, Shear buckling of orthotropic rectangular graphene sheet embedded in an elastic medium in thermal environment, *Composites Part B: Engineering*, Vol. 56, pp. 629-637, 2014.
- [34] M. Mohammadi, A. Moradi, M. Ghayour, A. Farajpour, Exact solution for thermo-mechanical vibration of orthotropic mono-layer graphene sheet embedded in an elastic medium, *Latin American Journal of Solids and Structures*, Vol. 11, pp. 437-458, 2014.
- [35] M. Mohammadi, A. Farajpour, M. Goodarzi, F. Dinari, Thermo-mechanical vibration analysis of annular and circular graphene sheet embedded in an elastic medium, *Latin American Journal of Solids and Structures*, Vol. 11, pp. 659-682, 2014.

- [36] M. Mohammadi, A. Farajpour, M. Goodarzi, Numerical study of the effect of shear in-plane load on the vibration analysis of graphene sheet embedded in an elastic medium, *Computational Materials Science*, Vol. 82, pp. 510-520, 2014.
- [37] A. Farajpour, A. Rastgoo, M. Mohammadi, Surface effects on the mechanical characteristics of microtubule networks in living cells, *Mechanics Research Communications*, Vol. 57, pp. 18-26, 2014.
- [38] S. R. Asemi, M. Mohammadi, A. Farajpour, A study on the nonlinear stability of orthotropic single-layered graphene sheet based on nonlocal elasticity theory, *Latin American Journal of Solids and Structures*, Vol. 11, pp. 1541-1546, 2014.
- [39] M. Goodarzi, M. Mohammadi, A. Farajpour, M. Khooran, Investigation of the effect of pre-stressed on vibration frequency of rectangular nanoplate based on a visco-Pasternak foundation, 2014.
- [40] S. Asemi, A. Farajpour, H. Asemi, M. Mohammadi, Influence of initial stress on the vibration of double-piezoelectric-nanoplate systems with various boundary conditions using DQM, *Physica E: Low-dimensional Systems and Nanostructures*, Vol. 63, pp. 169-179, 2014.
- [41] S. Asemi, A. Farajpour, M. Mohammadi, Nonlinear vibration analysis of piezoelectric nanoelectromechanical resonators based on nonlocal elasticity theory, *Composite Structures*, Vol. 116, pp. 703-712, 2014.
- [42] M. Mohammadi, M. Ghayour, A. Farajpour, Free transverse vibration analysis of circular and annular graphene sheets with various boundary conditions using the nonlocal continuum plate model, *Composites Part B: Engineering*, Vol. 45, No. 1, pp. 32-42, 2013.
- [43] M. Mohammadi, M. Goodarzi, M. Ghayour, A. Farajpour, Influence of in-plane pre-load on the vibration frequency of circular graphene sheet via nonlocal continuum theory, *Composites Part B: Engineering*, Vol. 51, pp. 121-129, 2013.
- [44] M. Mohammadi, A. Farajpour, M. Goodarzi, R. Heydarshenas, Levy type solution for nonlocal thermo-mechanical vibration of orthotropic mono-layer graphene sheet embedded in an elastic medium, *Journal of Solid Mechanics*, Vol. 5, No. 2, pp. 116-132, 2013.
- [45] M. Mohammadi, A. Farajpour, M. Goodarzi, H. Mohammadi, Temperature Effect on Vibration Analysis of Annular Graphene Sheet Embedded on Visco-Pasternak Foundati, *Journal of Solid Mechanics*, Vol. 5, No. 3, pp. 305-323, 2013.
- [46] A. Farajpour, A. Shahidi, M. Mohammadi, M. Mahzoon, Buckling of orthotropic micro/nanoscale plates under linearly varying in-plane load via nonlocal continuum mechanics, *Composite Structures*, Vol. 94, No. 5, pp. 1605-1615, 2012.
- [47] M. Mohammadi, M. Goodarzi, M. Ghayour, S. Alivand, Small scale effect on the vibration of orthotropic plates embedded in an elastic medium and under biaxial in-plane pre-load via nonlocal elasticity theory, 2012.
- [48] A. Farajpour, M. Mohammadi, A. Shahidi, M. Mahzoon, Axisymmetric buckling of the circular graphene sheets with the nonlocal continuum plate model, *Physica E: Low-dimensional Systems and Nanostructures*, Vol. 43, No. 10, pp. 1820-1825, 2011.
- [49] A. Farajpour, M. Danesh, M. Mohammadi, Buckling analysis of variable thickness nanoplates using nonlocal continuum mechanics, *Physica E: Low-dimensional Systems and Nanostructures*, Vol. 44, No. 3, pp. 719-727, 2011.
- [50] H. Moosavi, M. Mohammadi, A. Farajpour, S. Shahidi, Vibration analysis of nanorings using nonlocal continuum mechanics and shear deformable ring theory, *Physica E: Low-dimensional Systems and Nanostructures*, Vol. 44, No. 1, pp. 135-140, 2011.
- [51] M. Mohammadi, M. Ghayour, A. Farajpour, Analysis of free vibration sector plate based on elastic medium by using new version differential quadrature method, *Journal of solid mechanics in engineering*, Vol. 3, No. 2, pp. 47-56, 2011.
- [52] A. Farajpour, M. Mohammadi, M. Ghayour, Shear buckling of rectangular nanoplates embedded in elastic medium based on nonlocal elasticity theory, in *Proceeding of*, www.civilica.com/Paper-ISME19-ISME19_390.html, pp. 390.
- [53] M. Mohammadi, A. Farajpour, A. R. Shahidi, Higher order shear deformation theory for the buckling of orthotropic rectangular nanoplates using nonlocal elasticity, in *Proceeding of*, www.civilica.com/Paper-ISME19-ISME19_391.html, pp. 391.
- [54] M. Mohammadi, A. Farajpour, A. R. Shahidi, Effects of boundary conditions on the buckling of single-layered graphene sheets based on nonlocal elasticity, in *Proceeding of*, www.civilica.com/Paper-ISME19-ISME19_382.html, pp. 382.

- [55] M. Mohammadi, M. Ghayour, A. Farajpour, Using of new version integral differential method to analysis of free vibration orthotropic sector plate based on elastic medium, in *Proceeding of*, www.civilica.com/Paper-ISME19-ISME19_497.html, pp. 497.
- [56] N. Ghayour, A. Sedaghat, M. Mohammadi, Wave propagation approach to fluid filled submerged visco-elastic finite cylindrical shells, 2011.
- [57] M. Mohammadi, A. Farajpour, A. Rastgoo, Coriolis effects on the thermo-mechanical vibration analysis of the rotating multilayer piezoelectric nanobeam, *Acta Mechanica*, <https://doi.org/10.1007/s00707-022-03430-0>, 2023.
- [58] X. Luo, Z. Kuang, A study on the constitutive equation of blood, *Journal of biomechanics*, Vol. 25, No. 8, pp. 929-934, 1992.
- [59] Y. Liu, W. Liu, Blood flow analysis in tapered stenosed arteries with the influence of heat and mass transfer, *Journal of Applied Mathematics and Computing*, Vol. 63, No. 1, pp. 523-541, 2020.
- [60] H. Aminikhah, M. Hemmatnezhad, An efficient method for quadratic Riccati differential equation, *Communications in Nonlinear Science and Numerical Simulation*, Vol. 15, No. 4, pp. 835-839, 2010.
- [61] M. A. Ikbal, S. Chakravarty, K. K. Wong, J. Mazumdar, P. K. Mandal, Unsteady response of non-Newtonian blood flow through a stenosed artery in magnetic field, *Journal of Computational and Applied Mathematics*, Vol. 230, No. 1, pp. 243-259, 2009.
- [62] G. Varshney, V. Katiyar, S. Kumar, Effect of magnetic field on the blood flow in artery having multiple stenosis: a numerical study, *International Journal of Engineering, Science and Technology*, Vol. 2, No. 2, pp. 967-82, 2010.
- [63] H. Mirgolbabaee, S. Ledari, D. Ganji, Semi-analytical investigation on micropolar fluid flow and heat transfer in a permeable channel using AGM, *Journal of the Association of Arab Universities for Basic and Applied Sciences*, Vol. 24, pp. 213-222, 2017.
- [64] M. Mirzazadeh, Z. Ayati, New homotopy perturbation method for system of Burgers equations, *Alexandria Engineering Journal*, Vol. 55, No. 2, pp. 1619-1624, 2016.